National Library of Canada

Acquisitions and Bibliographic Services Branch

395 Wellington Street
Ottawa, Ontario
K1A 0N4

Bibliothèque nationale du Canada

Direction des acquisitions et des services bibliographiques

395, rue Wellington
Ottawa (Ontario)
K1A 0N4

Your file Votre référence

Our file Notre référence

NOTICE

The quality of this microform is heavily dependent upon the quality of the original thesis submitted for microfilming. Every effort has been made to ensure the highest quality of reproduction possible.

If pages are missing, contact the university which granted the degree.

Some pages may have indistinct print especially if the original pages were typed with a poor typewriter ribbon or if the university sent us an inferior photocopy.

Reproduction in full or in part of this microform is governed by the Canadian Copyright Act, R.S.C. 1970, c. C-30, and subsequent amendments.

AVIS

La qualité de cette microforme dépend grandement de la qualité de la thèse soumise au microfilmage. Nous avons tout fait pour assurer une qualité supérieure de reproduction.

S'il manque des pages, veuillez communiquer avec l'université qui a conféré le grade.

La qualité d'impression de certaines pages peut laisser à désirer, surtout si les pages originales ont été dactylographiées à l'aide d'un ruban usé ou si l'université nous a fait parvenir une photocopie de qualité inférieure.

La reproduction, même partielle, de cette microforme est soumise à la Loi canadienne sur le droit d'auteur, SRC 1970, c. C-30, et ses amendements subséquents.

Canada

OCULAR ARTIFACTS IN RECORDING EEGs AND EVENT RELATED POTENTIALS

Otavio G. Lins

Thesis presented to the School of Graduate Studies of the University of Ottawa as partial fulfillment of the requirements for the degree of Master of Sciences

Ottawa, Canada, July 29, 1993

ISBN 0-315-89675-2

Canada

UNIVERSITÉ D'OTTAWA
UNIVERSITY OF OTTAWA

ABSTRACT

The main goal of this work was to review and evaluate the different existent methods of compensating for ocular artifacts in recording the electrical activity from the brain. A related goal was to review and study the mechanisms that generate the potentials associated with blinks and eye movements.

The ocular artifacts derive from the potential difference between the cornea and the fundus of the eye. This can be represented by an equivalent dipole with its positive pole directed toward the cornea. The DC potential between the cornea and the forehead measures approximately +13 mV. The scalp-distribution of the ocular artifacts can be described in terms of propagation factors -- the percentage of the EOG present at the EEG electrodes. These factors are significantly different for blinks and upward eye-movements.

The source dipoles for blinks and saccades are different -- blink dipoles point radially whereas saccade dipoles point tangentially, in the direction of the eye movement. Blink and eye movement potentials are generated by different mechanisms -- blink potentials are generated by the eyelid sliding over the cornea, eye movement potentials by the rotation of the ocular dipole. A very small downward rotation of the eyes may occur during a normal blink. The "rider artifact" at the onset of upward saccade is caused by the eyelid as it lags behind the eyes at the beginning of the movement.

Smaller rider artifacts, caused by the horizontal asymmetry of the eyelid, can be noted during horizontal but not downward saccades.

Techniques that use scaled EOG to remove ocular artifacts from EEG recordings may remove some of the frontal EEG together with the ocular artifacts. Dipole source techniques allow the ocular generators to be distinguished from the nearby brain generators. A problem with dipole source techniques is that the head model used in the calculation is not accurate at the eyes. A new technique uses principal component analysis to estimate the ocular artifact at each electrode without using a head model. This technique is the most effective way to remove ocular artifacts from EEG recordings.

DEDICATION AND ACKNOWLEDGMENTS

I dedicate this work to

Terry Picton, more then my supervisor, a reference, scientifically and personally

Joana, my daughter,

Salustiano and Lucia, my parents

and Hiroko.

I am grateful to

Michael Scherg and Patrick Berg,

Yone, Sonya, Roberto, Silvia, Hiroe, Hiroko, Terry, Miho, Michele, Adrian, Manon, José, Sandra, Linda, Wayne, Hans, Janet, Jag, Francisco, Beatriz, Dick, Magdi and Yuichiro, my subjects,

Wayne for talking about statistics and proof reading,

Michele, Marty and Corinne for proof reading,

Adrian for technical support,

Nathalie, Dr. Ken Marshall and Dr. David Parry.

All things...linked are,

That thou canst not stir a flower,

Without troubling of a star.

Francis Thompson

TABLE OF CONTENTS

LIST OF TABLES

LIST OF FIGURES

1

OVERVIEW

Electrical potentials generated by the eyes are often a serious problem when recording the electrical activity of the brain -- electroencephalography (EEG) and event-related potentials (ERP). Compared to the activity coming from the brain, some ocular artifacts often have high amplitudes. Ocular potentials occur in relation to movements of the eyelid (blinks, eyelid fluttering), movements of the eyes (saccadic and following eye movements), contraction of the extrinsic ocular muscles (lateral rectus spicule), stimulation of the retina by light (electroretinogram) and cerebral processes related to the visual system (lambda waves, "driving response" to light flashes).

In EEG and ERP recordings, potentials that do not originate from the brain are considered "artifacts" (Spehlmann 1981). Ocular artifacts can make the interpretation of the EEG waveforms from anterior regions of the brain very difficult since they can mimic normal or abnormal cerebral electric activity (Spehlmann 1981, Brittenham 1990). For ERP recordings, ocular artifacts may distort the averaged waveform because they are easily driven by the stimuli (Hillyard and Galambos 1970; Picton 1987). Since they can have large amplitudes, they may be hard to remove by averaging, even when they are not time-locked to the stimuli. Ocular artifacts are a particular problem for computerized analysis of EEG, since current algorithms cannot easily distinguish brain potentials from eye potentials (Lee and Bushsbaum 1987).

The origin of the ocular potentials

A recording of ocular potentials associated with eye movements from electrodes near the eyes is known as the electro-oculogram (EOG) (Marg 1951). The EOG was first recorded by Meyers (1929) and Jacobson (1930). They proposed that these potentials were generated in the extrinsic ocular muscles. A few years later Mowrer et al. (1936) disproved this proposal by showing that similar potentials could be recorded during passive movements of the eyes of an anesthetized cat. They proposed that the potentials derived from movements of the electrical fields of the eyes. The existence of an electrical potential difference between the cornea and the fundus of the eye was demonstrated by du Bois-Reymond in 1849 by recording this corneofundal (or corneoretinal) potential from the eye of a freshwater carp. In vertebrates the cornea is positive and the fundus negative while in invertebrates the cornea is negative and the fundus positive. The corneofundal potential is generated primarily by the retina, between the sclera and the vitreous (Steinberg et al. 1983). In vertebrates the vitreous side of the retina is positive and the scleral side negative while in invertebrates the vitreous side is negative and the scleral side positive (Marg 1951). The photoreceptor cells in the vertebrates retina point outwards whereas in invertebrates they point inwards (Moses 1970). There are great discrepancies among the reported magnitudes of the corneofundal potential. It has been described as from about 1 mV (Barber 1980; Davson, 1990) to about 100 mV (Kiloh et al. 1981; Fisch 1991). With exposure to light the potential initially increases over a period of 10 to 15 minutes to a level that is two or more times larger than in the dark-adapted eye (Arden et al. 1962; Arden and Barrada 1962; Arden and Kelsey 1982). After this initial "light rise", the potential oscillates and reaches a stable level after about 90 minutes. These fluctuations are probably related to ionic currents in the retina. For conjugate lateral movements, the potentials recorded between the left and right external canthi are linearly related to the size of the eye movement (Geddes and Baker 1989). Measuring the EOG as the eyes move

through standardized angles can provide a non-invasive indirect estimate of retinal function (Arden et al. 1962a; Berson, 1987). The EOG is also used to measure eye movements in electro-nystagmography (Barber, 1980; Coats, 1975) and to monitor eye movements in polygraphic recordings of sleep (Rechtschaffen and Kales 1968, Carskadon and Rechtschaffen 1989).

A separation of charges in space, positive in one location and negative in another, can be represented by a dipole. A dipole is defined by its location, orientation and magnitude. The three-dimensional location of a dipole is defined by three numbers, the orientation represented by two numbers and the magnitude (or strength) represented by one number. A dipole, thus, can be completely defined by six variables. Dipoles are graphically represented by arrows. The origin of the arrow is the dipole location, the direction where the arrow points is the orientation and the size of the arrow is the strength. The retina is shaped like a cup or an open sphere. The sum of all the smaller retinal dipoles can be represented by an equivalent dipole located close to the center of the eyeball. In vertebrates, the positive side of this equivalent dipole is oriented toward the opening of the sphere at the cornea, in approximately the direction of gaze.

In addition to the retina other generators probably also contribute to the corneoretinal potential. There is a potential difference between the interior of the lens and its surroundings and between the front and the back of the lens (Brindley 1956). There is also a potential difference across the cornea, between the aqueous fluid and the tears (Donn et al. 1959). Perhaps most importantly, there is a significant Gibbs-Donnan equilibrium potential between the blood and the aqueous humor (Müller-Limmroth and Lemaître 1953). That is probably the reason why one can still record some EOG after ablation of the retina (Pasik et al. 1965).

Eye movement potentials

The mechanisms that generate eye movement potentials are fairly well understood. When the eyes move, the regions of the head toward which the positively charged cornea moves become more positive and the regions of the head toward which the negatively charged fundus moves become more negative. As previously discussed, the corneofundal equivalent dipole points approximately toward the direction of gaze. If the eyes are stationary, no effects from these dipoles are recorded from surface electrodes by recording systems that use capacitor-coupled amplifiers, high-pass filters or baseline compensation procedures. When the eyes move, the orientation, and to a smaller extent the location of the corneofundal dipoles changes in relation to the head. It is these *changes* that are registered by the recording systems rather than the resting potentials.

The changes in electrical fields generated by rotation of the ocular equivalent dipoles can also be represented by dipoles. These *differential* dipoles will be equal to the vector difference between the starting and ending positions of the ocular equivalent dipoles. The magnitude of the differential dipoles will be larger with larger rotation of the eyes. Without considering the small change in location of the ocular equivalent dipoles that may occur during the rotation of the eyes, the location of the differential dipoles will be the same as the ocular equivalent dipoles. The orientation of the differential dipoles will depend on the way the eyes move. Starting from looking straight ahead, if the eyes move upward the differential dipoles will point up, if the eyes move downward the dipoles will point down and so on. A more subtle effect on the orientation of the differential dipoles will be produced by the magnitude of the eye movement: The larger the rotation the more the differential dipoles will point backward (as well as in the direction of the eye movement).

Blink potentials

In contrast to eye movements, the mechanisms that generate the potentials associated with blinking are not clearly understood. There are basically two hypotheses:

The first hypothesis is based on Bell's phenomenon (Wilkins and Brody 1969). A patient with a peripheral lesion of the facial nerve cannot close the eyes completely on the affected side because of palsy of the facial muscles. On attempting to close the eyes, the eyeball will move upwards, a normal phenomenon that becomes visible because of the incomplete eye closure (Brazis et al 1990). The Bell's phenomenon hypothesis, thus, states that blinking is also associated with an upward rotation of the eyes (Hector 1976; Kiloh et at 1981). If this hypothesis is true it would mean that blink potentials are generated by the same mechanism as upward eye movement. Blink dipoles should, thus, be similar to upward eye movement dipoles, that is, they should be oriented upward.

The second hypothesis states that blink potentials are generated simply by the movement of the eyelid over the cornea. The eyelid would act as a sliding electrode connecting the scalp to the positively charged cornea (Matsuo et al 1975). If the sliding electrode hypothesis is true, blink potentials would be generated by a mechanism different from that producing the eye movement potentials. As the eyelid slides over the positively charged cornea the flow of current through the lid increases, without any change in the orientation of the corneo-retinal dipoles. The net orientation of the resultant dipole expressing the net current flow during the movement of the lid down the cornea would be oriented forward.

Several electrophysiologic studies have suggested that different mechanisms generate blink and eye movement potentials. Blinks and vertical eye movements potentials

propagate differently across the head. Vertical eye movement propagates further back on the scalp than blinks (Hillyard and Galambos 1970, Corby et al. 1972). Upward eye movements produce a positivity above the eye and a negativity of similar magnitude below the eye whereas blinks produce a larger positivity above the eye than the negativity below the eye (Zao et al. 1952; Antervo et al. 1985; Berg and Scherg 1991a). Studies using dipole modeling techniques (Berg and Scherg 1991a, 1991b) have shown that blink dipoles point forward, as the sliding electrode hypothesis predicts.

More direct studies have failed to show significant upward eye movements during normal blinks. Doane (1980), using a high-speed photographic system, found no significant upward eye movement during normal blinks in human subjects. If the blinks were strong and forced, or if the upper eyelid was restrained, an upward rotation was noted. Collewijn et al (1985) studied blinks in human subjects using coils attached to the conjunctiva in a magnetic field. They found that blinks were consistently associated with a one to five degrees downward and nasalward rotation of the eyeballs. Prolonged closure of the eyelids was associated with a slow, tonic upward eye rotation of the eyes in half of the subjects and a downward rotation in the other half.

Other eye-related potentials

Several other potentials can occur in addition to those caused by the movement of the eye or the eyelid. These can be generated in the ocular muscles, the retina and the brain.

The ocular muscles generate potentials that can be recorded from the scalp. The lateral rectus spicules (Blinn 1955) have been recognized for a long time in raw EEG tracings. They probably represent the synchronized activation of fibers in the lateral rectus

at the beginning of a lateral saccade. Other smaller potentials may occur during the continuation of the eye-movement, but because of desynchronization these would be much smaller than the potentials at the onset. Other ocular muscles may also generate recordable potentials, but these would be small since they are further away from recording electrodes than the lateral rectus.

The retina may generate potentials that are associated with changes in the position of the eye or the eyelid. These potentials would be generated by the retina's response to the changing visual input. These responses would be very small and difficult to disentangle from the potentials related to the rotation of the eye or the closure of the eyelid.

Three basic kinds of cerebral potentials can occur in association with eye-movements and blinks. The first are those potentials related to motor control. These could be generated by both cortex and subcortical structures, and would vary with the nature of the eye movement (voluntary or automatic) and the state of arousal. Kurtzberg and Vaughan (1982) described a slow parietal negativity that culminated in a sharp positive wave immediately before the onset of a saccade. The second type of cerebral potential associated with eye-movements can occur with the processing of new sensory input. Following a saccade, there is an occipital positive wave -- the lambda wave -- that probably represents the evoked potential to the changed visual input (Yagi 1981). The waves that follow saccades during wakefulness are different from those that follow rapid-eye-movements of sleep (Miyauchi et al. 1987). The small occipital positive potentials that occur about 300 ms after the onset of a blink may represent a lambda-like evoked potential to the brief change in visual input during the blink, particularly the reinstatement of the visual field at the end of the blink (Berg 1986; Berg and Davies 1988). Late endogenous positive waves may occur in relation to information-processing when the saccades fix on a meaningful visual stimulus (Marton et al. 1985). A third kind of cerebral potential

associated with eye-movements may be related to "efference copy" or "corollary discharge" (McCloskey 1981). This process affects sensory analysis in anticipation of the change in visual input that will result from the eye-movement being initiated. Such a process would ensure a smooth perception of the visual world despite the jerkiness and intermittence of the visual input.

Eye-related potentials can provide us with important information concerning visual perception. They can only be studied if we have adequate techniques to disentangle them from the potentials that are associated with the actual movements of the eye or eyelid.

Ways to reduce eye movement and blink artifacts

There are several ways to reduce the amount of ocular artifact in a recording. The most obvious is to ask the subject not to blink or move the eyes during the recording session. Periods of blinking or eye movement are eliminated from the analysis. However, there are several problems with this approach. First, it may be difficult or even impossible for some subjects (children, psychiatric patients) to refrain from blinking or moving their eyes. The ocular artifacts may occur during most of the recording making it impossible to obtain an acceptable sample for analysis or averaging. Second, some ocular potentials may be too small to be recognized but yet be sufficiently time-locked to the stimuli to significantly distort the averaged data (Picton 1987). Third, periods with high and low blink rates may be associated with different functional cerebral states (Stern et al. 1984). A related problem is that a person who has to pay attention to not blinking or moving his or her eyes may not pay as much attention to the main task of the experiment as a person who ignores this behaviors (Verleger 1991). Fourth, eye movements may be an integral part of the paradigm. For example, in experiments that use auditory event-related

potentials to study attention reading is often used in the conditions in which the experimenter does not want the subject to pay attention to the auditory stimuli.

There are several techniques to remove the ocular artifacts from recordings, after they have occurred. A common assumption of these techniques is that the EEG signal recorded at the scalp is composed of a EEG signal (brain activity) plus an ocular artifact:

$$EEG_{RECORDED} = EEG + OCULAR\ ARTIFACT$$

If one subtracts the ocular artifact from the scalp recorded EEG a "corrected" EEG will be obtained.

$$EEG = EEG_{RECORDED} - OCULAR\ ARTIFACT$$

The ocular artifact recorded at each electrode site will depend on the position of the recording electrodes in relation with the eyes. Since ocular potentials propagate across the scalp by volume conduction and the electrical conductance of the head tissues is finite, the ocular potentials will be smaller as the distance between the eyes and the recording sites increases. Furthermore, the recorded ocular potentials will also depend on the spatial location of the recording electrode in relation to the eyes. For example, ocular potentials produced by blinks and vertical eye movements will be larger at electrodes situated at midsagittal locations than at temporal positions. Conversely, for horizontal eyes movements, electrodes at temporal locations will detect larger ocular potentials than electrodes at midsagital positions. The amount of ocular potential that reaches each scalp recording electrode will, thus, be some fraction of the ocular activity. This fraction will be the ocular activity scaled by a "propagation factor", the value of which will depend on the location of the recording electrode at the scalp, i.e.,

OCULAR ARTIFACT = PROPAGATION FACTOR × OCULAR ACTIVITY

An important assumption of this approach is that the ocular artifact at the EEG electrodes is a linear function of the ocular activity. Hillyard and Galambos (1970) demonstrated that this fraction is reasonably stable over eye movement of up to 15 degrees. Some authors have proposed that the head acts as a low-pass filter causing the spread of the ocular potentials across the scalp to vary with frequency (Whitton et al. 1978; Gasser at al. 1986). However, this variation with frequency is not significant at frequencies below 5 Hz where most of the EOG energy is concentrated (Berg's discussion in Brunia et al. 1989). Furthermore, the use of multiple propagation factors for each channel and each frequency band would increase the probability of sampling errors (discussion by Gratton and Coles in Brunia et al. 1989). The observed frequency differences may result from the mixture of both blinks and eye movements in the EOG signal since blinks have both a faster frequency and a smaller field-spread. They may also have been related to the EOG monitor recording frontal EEG signals as well as EOG

Therefore, to eliminate ocular artifacts from EEG (or ERP) recordings one must have some estimate of the ocular activity and propagation factors that describe how much of this ocular activity is recorded at each particular recording site. This may be expressed as follows:

$EEG = EEG_{RECORDED}$ - (PROPAGATION FACTOR × OCULAR ACTIVITY)

The EOG as an estimate of the ocular activity

The easiest way to estimate ocular activity is to record the EOG from electrodes placed around the eyes. As eye movements can have vertical, horizontal and diagonal components, it is necessary to record both vertical and horizontal EOGs. The vertical EOG is recorded from electrodes above and below the eyes and the horizontal EOG from electrodes at each side of the eyes. Since the field changes in blinks are basically forward and a little upward, the vertical EOG is sufficient to estimate blink electrical activity. If one just wants to correct recording from midsagittal electrodes, a single vertical EOG channel is sufficient for both blinks and eye movements (Barlow 1986). The next step is to obtain the fractions of the EOG that contaminate the EEG from each scalp recording site. This can be done using analog techniques or digital techniques. Analog techniques use continuous signals and can be very simple or quite complex. McCallum and Walter (1968) used the center tap of a potentiometer as a balanced reference between a frontal electrode and an electrode at the mastoid. By adjusting the center tap of the potentiometer they could adjust the proportion of the EOG subtracted from the recorded signal. Barlow and Remond (1981) used a more complex multichannel electronic device to perform the subtraction. The advent of powerful and relatively inexpensive computers made digital techniques much more flexible and efficient (Jervis et al. 1985). These techniques use digitized signals and computer programs to calculate propagation factors, scale the EOG to obtain the fractions of the EOG at the EEG electrodes and subtract these fractions from the EEG (Jervis et al. 1988, Ifeachor et al, 1988). The propagation factors can be calculated simply by dividing the peak voltage of the ocular potentials at each EEG channel and at the EOG channels. However, this procedure uses only one data point and large inaccuracies can occur, especially at more posterior electrode sites where the amplitude of the ocular artifacts is rather small. It is much more efficient to calculate the propagation factors by performing a linear regression

between the digitized data points of the EOG channels and the data points recorded at each EEG electrode site. The propagation factors are then the slopes of the best-fit straight lines of the regression equations (Hillyard and Galambos 1970). The propagation factors are used to scale the EOG signal in order to obtain the proportion of the EOG that reaches each recording site. The scaled EOG signals are then subtracted from the signals recorded at each recording site.

As considered in previous paragraphs, eye movement and blink potentials have different field-spreads across the scalp. Eye movement propagation factors tend to be larger than blink propagation factors at more posterior regions of the scalp. If, for example, one corrects blinks with eye movement propagation factors, the blinks would tend to be overcompensated at the more posterior electrode positions. If, on the other hand, one corrects eye movements with blink propagation factors, eye movements would tend to be undercompensated at more posterior electrode sites. Therefore, separate propagation factors should be calculated for eye movements and blinks (Gratton et al. 1983). Elbert et al. (1985) proposed a third EOG monitoring channel to record the radial component of the EOG signal. Three propagation factors could then be calculated, allowing blinks and upward eye movements to be differentially compensated. Gratton used a two-step method to correct the recordings for blinks and eye movements. Blinks were identified by locating the time points where the rate of change of the EOG exceeded a set criterion. Blink propagation factors were calculated around those time points, and all the activity in the epoch was corrected using the blink propagation factors. Eye movement propagation factors are calculated using the data remaining after the blinks had been corrected. Finally, the data were again corrected using the eye movement propagation factors. Gratton's method calculates the propagation factors from the actual data obtained during the experiment. This approach would have the advantage of being less affected by fluctuations in the corneoretinal potential. However, the propagation factors are the

relative amounts of the EOG that propagate to each recording site at the scalp, since this quantity is calculated in relation to the EOG. Consequently, they should not be significantly affected by fluctuations in the amplitude of the corneoretinal potential. The method has some disadvantages. All single trials need to be stored for later analysis and this could demand a large amount of computer memory. Furthermore, the correction procedure is performed off-line thereby making the corrections more time-consuming. The propagation factors can also be calculated from calibration trials obtained prior to the experiment. During these trials, the subject performs blinks and standard eye movements of a given angular magnitude. The propagation factors are then calculated from these calibration trials and used on-line to correct the recordings. However, the use of the EOG as an estimate of ocular activity is problematic. What is really recorded at the EOG channels are the ocular potentials plus some EEG activity, generated mainly in the frontal regions of the brain:

$$\text{EOG}_{\text{RECORDED}} = \text{OCULAR ACTIVITY} + \text{EEG}$$

This leads to at least two problems. First, the linear regression may give incorrect slopes and thus incorrect propagation factors as the brain activity has a different scalp-distribution than the ocular activity. Second, and most important, in the subtraction procedure the frontal EEG activity picked up by the EOG channels will be partially subtracted out from the scalp-recordings (Berg and Scherg 1991b; Berg et al. 1993):

$$\text{EEG} = \text{EEG}_{\text{RECORDED}} - [\text{PROPAGATION FACTOR} \times (\text{OCULAR ACTIVITY} + \text{EEG}_{\text{FRONTAL}})]$$

A surface electrode records the activity of all generators (or sources) that are active during the recording period and that generate fields at the surface of the head. If there are several

sources, the surface recorded waveforms will be more complex than the waveforms from each source. The EOG therefore is not a "true" estimate of the ocular activity because: (1) activity from the brain is also picked up by the EOG electrodes; and, (2) the ocular potentials themselves are generated by more then one mechanism. The first problem can be partially attenuated by calculating the factors using eye movements of large amplitude and/or averaging the eye movements to reduce the EEG. The second problem can be partially attenuated by calculating different propagation factors for each source (for example, for blinks and vertical eye movements) and correcting each type of ocular artifact separately. However, if multiple sources are active at the same time (for example, a blink during a vertical eye movement) it will be impossible not to overcompensate or undercompensate the artifact in regions of the head where the propagation pattern of the sources differs (for example, in posterior regions of the head for blinks and vertical eye movements).

Source dipoles as an estimate of ocular activity

A new technique, Brain Electric Source Analysis (BESA) (Scherg and von Cramon 1985, 1986; Scherg 1990; Scherg and Picton 1991; Scherg in press), may help to overcome these difficulties. This technique models the sources that underlie scalp recorded waveforms. The calculation of the activity at the surface of the head generated by a number of intracranial sources in known as the *forward problem*. Conversely, the calculation of the locations, orientations, and activity of the intracranial sources from scalp-recorded waveforms is know as the *inverse problem*.

$$\text{SOURCE ACTIVITY} \underset{\text{INVERSE PROBLEM}}{\overset{\text{FORWARD PROBLEM}}{\rightleftarrows}} \text{SCALP ACTIVITY}$$

The forward problem

Considering only one intracranial source, electrodes at the surface of the head will record the activity of the source scaled by a propagation factor that accounts for the transfer of the activity of the source to the recording electrodes.

$$\text{ACTIVITY}_{\text{ELECTRODE}} = \text{PROPAGATION FACTOR} \times \text{ACTIVITY}_{\text{SOURCE}}$$

The propagation factor will depend on the distance between the source and the electrodes and on how the source is spatially oriented relative to the electrodes. It will also depend on the conductance characteristics of the head which is composed of tissues of different electrical conductances. This can be described by a mathematical head model. Present computer programs use a simplified three-shell spherical head model accounting for the brain, the skull, and the scalp conductances (Scherg 1990, Scherg and Picton 1991).

$$\text{PROPAGATION FACTOR} = f(\text{SOURCE}_{\text{LOCATION, ORIENTATION}} ; \text{HEAD MODEL})$$

With **n** sources (S), the activity recorded by each electrode will be the linear sum of the activity of all n sources (principle of superposition).

$$\text{ACTIVITY}_{\text{ELECTRODE}} = \sum_{S=1}^{n} (\text{PROPAGATION FACTOR}_S \times \text{ACTIVITY}_S)$$

The inverse problem

The BESA program does not directly perform an inverse calculation but, as will be described shortly, calculates the forward solution for an initial set of sources and then iteratively changes the location and orientation of the sources with the goal of finding the configuration of sources that generates surface activity that most precisely fits the recorded data. Theoretically, there is no unique solution for the inverse problem. However, approximate unique solutions do exist if the number of possible solutions is limited by establishing "constraints" from prior anatomical and physiological knowledge and a large number of recording channels in relation to the number of postulated sources are used.

Traditional dipole source analysis techniques model the sources for only one time point at a time (Fender 1987). The BESA technique uses all the data points of a given epoch to model not only the locations and orientations of the sources, but also the activity of the sources over time. This "spatio-temporal approach" further decreases the number of possible solutions. Perhaps more importantly, it provides an opportunity to visualize not only where the sources are inside the head, but also when and how they are active during the period recorded.

The BESA algorithm works in four steps: Step 1: An initial model is postulated. The number of sources, their locations and orientations, as well as other constraints are decided using prior knowledge and logical reasoning based on the hypothesis been tested. For example, to model blinks or eye movements it would be reasonable to start with two dipoles located at the eyes. Some symmetry between the two sources would also be expected; Step 2: The program calculates the corresponding model waveforms for each electrode site using the transfer functions derived from the head

model. As previously shown, this forward computation has a unique solution; Step 3: The program compares the modeled waveforms with the recorded waveforms. This is done by calculating the "residual variance", a measure of how the modeled waveforms *differs* from the recorded waveforms. A small residual variance means that the model fits the data well; and Step 4: The program alters the model by changing the locations and orientations of the dipoles. Then step 2 is repeated.

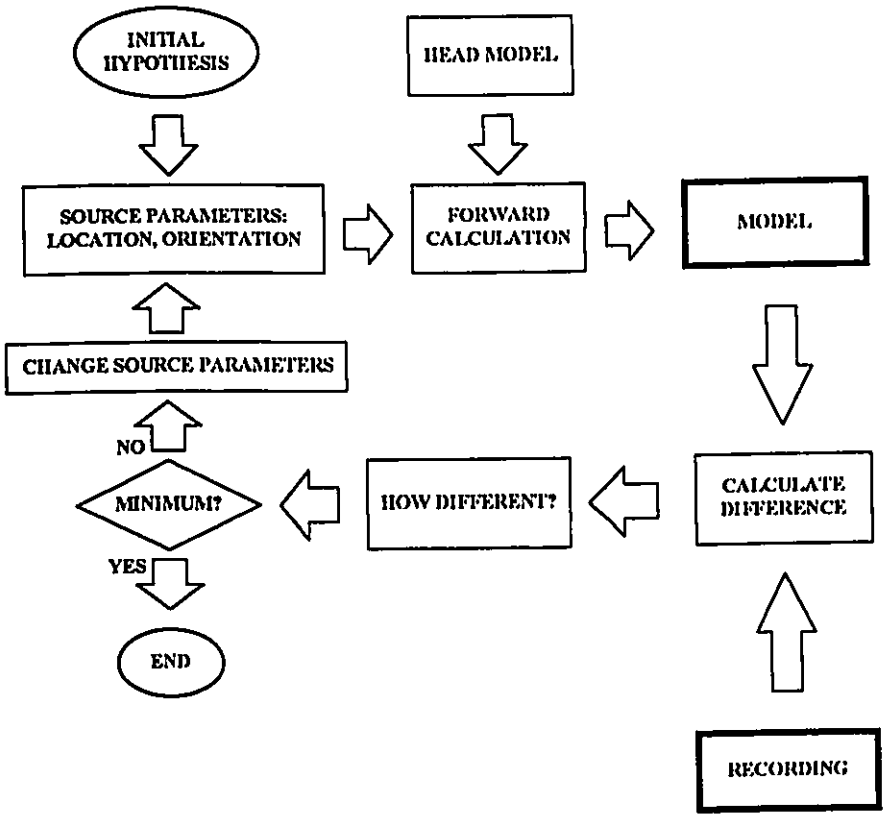

This cycle repeats with the program attempting to minimize the residual variance and, thus, obtain a better correspondence between the model and the data. The "best-fit" model, if physiologically reasonable, is accepted as the solution for those data.

BESA can be used to correct ocular artifacts. The general idea is to use source dipoles to model both ocular and brain activity. The ocular dipoles are either maintained in the general model (if working with BESA) or their activities are subtracted from the recorded data to obtain a corrected data set that can be used for other applications. To separate the ocular activity from the brain activity both have to be included at the same model. The brain activity can be modeled in two ways (Berg and Scherg 1993): (1) by actually modelling the brain sources; or; (2) by using several regional sources (a set of three orthogonal dipoles with the same location) placed in strategic positions in the head. Although the regional sources are not located at the exact locations of the EEG sources they would be close enough to them to be able to model most of the brain activity.

Source dipoles are better estimates of ocular activity than the EOG. Instead of surface recorded potentials that combine both ocular and brain activities, the dipoles represent the actual ocular sources. However, the method has some problems related with the use of a head model. First, the ocular sources are very near the surface of the head and the electrical fields there are very steep. This makes the positioning of the electrodes near the eyes very critical. Small inaccuracies in electrode positioning with respect to the model will have large effects. Second, the simplified three-shell head model used in BESA is inaccurate for the eyes. The eyes are located inside a boney socket, open to the outside. This leads to inaccurate source dipoles for the ocular potentials.

Source components as an estimate of ocular activity

Ocular activity can be estimated without the constraints of head models using Principal Component Analysis (PCA). Although source dipole modelling is based in a more "physiological" concept, the PCA technique may work better for the purpose of

removing ocular artifacts. PCA decomposes a set of variables into orthogonal (independent) subsets. Variables that are correlated with one another (but independent of other variables) are combined into components. The components are thought to reflect the underlying processes that have created the correlations among variables (Tabachnick and Fidell 1989; Gevins 1987; John et al. 1987; Möcks and Verleger 1991). If the variables are significantly correlated, the first few components will account for most of the variance of the data.

Berg, Scherg and others (Berg and Scherg 1991b, Berg et al. 1993) used a technique based on PCA for correction of artifacts. First, a set of calibration recordings is obtained by recording while the subject performs blinks and relatively large eye movements. Second, the brain activity is modelled with source dipoles. As with the source dipoles correction method, this can be done by actually modelling the brain activity or by using regional sources placed in strategic positions in the head. Third, a PCA of the calibration recording is performed in the presence of the brain activity source dipoles. The brain activity source dipoles are used to "separate" the brain activity from the ocular activity. The ocular activity resulting from blinks and large eye movements is of a much larger amplitude than the brain activity. As a result, the main components of the PCA will be generally related to the blinks and eye movements or some linear combination thereof. Berg and Scherg (1991b) used three components, basically related to blinks, vertical and horizontal eye-movements. Fourth, the ocular activity present at each electrode location is estimated using the ocular components. Fifth, The ocular activity is subtracted from the raw EEG to obtain a corrected EEG.

2

SCALP TOPOGRAPHY

INTRODUCTION

The potentials associated with blinking or moving the eyes derive from the potential difference between the cornea and the fundus of the eye. The reported magnitude of this corneofundal potential varies widely: from 1 to 100 mV. The corneofundal potential is generated basically across the retina, a cup-shaped structure positive on the inside and negative the outside. The resultant separation of charges can be approximated by a dipole at the center of the eye with its positive pole oriented in the direction of gaze. Eye movement potentials are generated by the rotation of the corneofundal dipoles. Blink potentials are less well understood but most probably are generated by the eyelid sliding over the positively charged cornea.

The scalp topography of the potentials generated by blinks and eye movements can be described in terms of propagation factors. These factors measure the percentage of the potential recorded in EOG electrodes that is picked up at a particular scalp location. Eye movement potentials need two sets of propagation factors: vertical and horizontal. A separate set of vertical propagation factors is needed for blinks.

In this chapter, the DC potentials from the cornea, conjunctiva, and skin adjacent to the eyes and the scalp topography of blink and eye movement potentials are evaluated.

METHODS

Experimental design

Fourteen female and 9 male subjects ranging in age from 13 to 47 (mean 32) years participated in three experiments. All subjects were healthy and had no history of ophthalmologic problems (other than refractive errors) or neurologic disease.

(i) **First experiment**. In this experiment the DC potentials from the cornea, conjunctiva and adjacent regions of the skin were mapped using wick electrodes. Three subjects, all male, participated in these recordings. The subjects lay on a bed and held a wick electrode on their own cornea, conjunctiva, and face using a mirror for guidance.

(ii) **Second experiment**. This study was designed to study how the ocular potentials propagate across the scalp. Twelve subjects (7 female) participated in this experiment. There were no significant differences between the ages of the male and female subjects (male 34±8, female 31±8), although these groups were not formally matched for age. For the recordings of the second and third experiments, the subjects sat in a comfortable chair in an electrically shielded and sound-attenuated room. A board placed 80 cm in front of the subjects displayed multiple numbered black dots showing the desired angular deflections (10° or 20°) for the saccades and a central fixation point. Blinks were studied under 2 conditions: "natural" and "voluntary". For *natural blinks*, subjects fixated their eyes at the center dot of the board and repeated recordings were obtained until several blinks occurred. For *voluntary blinks* the subjects were asked to blink about once every one to two seconds. *Saccades* were studied for 2 excursions (20 and 10 degrees from the center point) and 8 directions (12:00, 1:30, 3:00, 4:30, 6:00, 7:30, 9:00 and 10:30 o'clock). Subjects fixated the center, then looked at one of the

labelled dots for about 2 seconds and then back at the center. To obtain *following eye movements* the subjects watched a tennis ball swinging on a string attached to the room's ceiling, without moving their heads.. The oscillation period of this pendulum was approximately 2.4 seconds and the excursion from 10° on one side to 10° on the other. Subjects were also recorded while *reading*. Two recordings were obtained for each of the experimental conditions.

(iii) **Third experiment**. The major goal of this experiment was to examine the source dipoles and source components underlying the EOG (see Chapter 2). A supplementary goal was to replicate the findings in the second experiment. Eight subjects (7 female) participated in this experiment. Activity was recorded during voluntary blinks and during 20-degree saccades in four directions (12:00, 3:00, 6:00 and 9:00 o'clock). Ten sweeps were obtained for each trial and subject.

Recordings

In the *first experiment*, wick electrodes (Geddes 1972) were used to record the direct-coupled (DC) potentials on the surface of the cornea and adjacent regions. Each electrode consisted of a Beckman Ag/AgCl electrode placed in a Plexiglas container filled with normal saline. A cotton wick connected the normal saline in the container to the recording location. The electrodes were kept short-circuited in a beaker of normal saline prior to use. The offset between electrodes varied from 0 to 2 mV and was stable with drifts of less than 0.5 mV per hour, provided that the wicks were kept moist. Inter-electrode impedance at 10 Hz was about 25 kOhms. Recordings were made using a reference at the vertex. The active recording locations were on the cornea, the conjunctiva, the forehead, the cheek and the mastoid. The recording location on the mastoid was scratched to connect the electrode to the subcutaneous tissue (Picton and

Hillyard 1972). The DC potentials between active and reference wick electrodes were amplified on a Grass 7P122B low-level DC amplifier and measured on a digital voltmeter after allowing the electrodes to stabilize for 30 s.

In the *second experiment*, gold-plated electrodes were fixed with collodion to the scalp and with adhesive tape to the skin. In this experiment, the vertical EOG (VEOG) was recorded between an electrode placed 1 cm above the supraorbital ridge and another placed 1 cm below the infraorbital ridge of the left orbit. (In supplementary recording sessions in 4 subjects, we also recorded the VEOG from the right eye.). The horizontal EOG (HEOG) was recorded between an electrode placed 2 cm lateral to the external canthus of the left eye and another 2 cm lateral to the right eye. For these sets of recordings the active electrode was the upper electrode for the VEOG and the left canthus for the HEOG. EEG electrodes were placed at Fp1, Fp2, F7, F3, Fz, F4, F8, A1, T3, C3, Cz, T4, A2, T5, P3, Pz, P4, T6, O1, Oz and O2. The EEG recordings were obtained on a Nicolet 1A97 EEG machine using a balanced noncephalic reference (Stephenson and Gibbs 1951). This reference electronically mimicked the center tap of a variable potentiometer linking electrodes placed over the right sternoclavicular junction and at the nape of the neck at the level of the C7 vertebra. Because the number of electrode locations being studied exceeded the sixteen channels of the recording system, two sets of recordings were made. The first set examined the anterior locations and the second set the posterior locations with the VEOG and HEOG, F7, Fz, F8, T3, Cz and T4 common to both sets.

To evaluate a larger population of subjects, blink and saccade scalp distributions were studied in 10 additional subjects (age 20 to 45 years) who were participating in a study of the auditory evoked potentials. In this study, scalp electrodes were located at F5, Fz, F6, M1, T3, C3, Cz, C4, P4, M2, P5, Pz, P6, and 0z (F5 was halfway between F3 and

F7, F6 between F4 and F8, P5 between P3 and T5, P6 between P4 and T6). These were referred to a noncephalic reference. The vertical and horizontal EOG was recorded as described in the previous paragraph.

For the *third* experiment, electrodes were placed around the eyes (above and below both left and right eyes, lateral to the external canthi and at the nasion) and at several head positions (Fz, A1, T3, C3, Cz, C4, T4, A2 and Pz). Both EOG and EEG electrodes were referred to the noncephalic reference.

Electrode impedances in the second and third experiments were kept below 3 kOhms. The on-line analog filter bandpass was 0.15 to 70 Hz (-3 dB points, slope 6 dB/octave for the low frequencies and 12 dB/octave for the high). Data were digitized at 200 Hz using sweeps of 5120 ms on a 386 IBM-PC clone computer equipped with a Data Translation A/D board.

Measurements

Three *head measurements* were taken: the inion-nasion distance, the distance between the left and right preauricular points, and the circumference at the level of Oz and Fpz.

Five *blink measurements* were obtained from the vertical EOG channel: peak amplitude, total duration, onset-to-peak duration, peak-to-end duration and half-amplitude duration (duration between the half-amplitude point before the peak and the half-amplitude point after the peak). The algorithm to obtain the onset and the end of a blink found the peak of the blink and then moved in both directions until the amplitude returned

to within the range of the baseline EOG recorded during fixation. Durations were measured in ms and amplitude in μV.

The *slopes* of the natural and voluntary blinks and the saccades were calculated. The blinks were measured for both onset and offset whereas the saccades were only measured on their initial onset. Slopes were expressed in μV/ms. The rate of change of the slope in $\mu V/ms^2$ was also measured by calculating the amplitude changes before and after the peak of the deflection over the following latencies: ±10, ±20, ±50, and ±100 ms.

EOG *propagation factors* were calculated by linear regression as the slopes of the best-fit straight lines relating the EOG with the EEG signal at any particular electrode location (Hillyard and Galambos 1970). To simplify the tables and text, these factors are referred to as percentages rather than ratios (e.g., 5% rather than 0.05). The time periods over which the blink propagation factors were calculated lasted from about 100 msec before blink-onset to between 200 and 300 msec after the end of the blink in the VEOG channel. The propagation factors were calculated by a simple linear regression of the values recorded at a particular scalp-electrode with the values obtained on the EOG recording. Separate propagation factors were obtained for natural and voluntary blinks. For saccades, the periods evaluated were from about 100 msec before to 600 to 800 ms after the onset of the saccade in the VEOG and HEOG channel. Two propagation factors (vertical and horizontal) were calculated for saccades, using a multiple regression with two predictor variables. Separate propagation factors were obtained for 20° and 10° saccades with all directions combined, and then separately for up, down, left and right 20° saccades. The last four conditions were calculated using the 4 orthogonal directions plus the two oblique saccades forming 45° with them. The multiple regression procedure only worked well when the data set contained both vertical and horizontal eye movements. For the reading and following eye movements a simple regression was used and only the

horizontal propagation factors were calculated (A multiple regression could have been performed on some of the reading data which contained the vertical eye movements associated with a change of page but these trials were not frequent and the results were variable.).

Plotting conventions

The scalp-recorded data are all plotted negative up -- negativity at the scalp relative to the noncephalic reference is shown by an upward deflection.

Statistical Analyses

Occasional aberrant data that were more than 3 standard deviations from the mean were dropped from further analysis. T-tests were used to compare the duration and amplitudes for the two types of blinks and for the male and female groups. Repeated measures analyses of variance (ANOVA) with Greenhouse-Geisser adjusted degrees of freedom was used to compare the propagation factors. Pearson product-moment correlation coefficients were calculated to evaluate relations between head measurements and EOG features. A significance level of $p<0.05$ was used for all analyses.

RESULTS

Head size:

The average head-measurements are given in Table I. These measurements were slightly larger in males than females but these differences were not statistically significant.

Table I: Head measurements. All measurements are in centimeters

Measurement	Females	Males
Inion-nasion	34±2	36±2
Inter-Preauricular	35±2	37±2
Circumference	56±2	58±3

DC Potentials:

The average measurements from the wick-electrode recordings are shown in Table II. The data have been averaged across both eyes for all 3 subjects.

Table II: DC potentials recorded from the cornea, conjunctiva and adjacent skin areas. All measurements are in mV and are relative to the vertex.

Location	Resting Potential
Forehead	-14±9
Cheek	-10±6
Conjunctiva	-8±5
Cornea	-1±5
Mastoid (scratched)	+10±1

Blinks:

Typical natural and voluntary blinks, as recorded from the VEOG channel are presented in Figure 1. These were obtained by averaging blinks from all 12 subjects who participated in the second experiment.

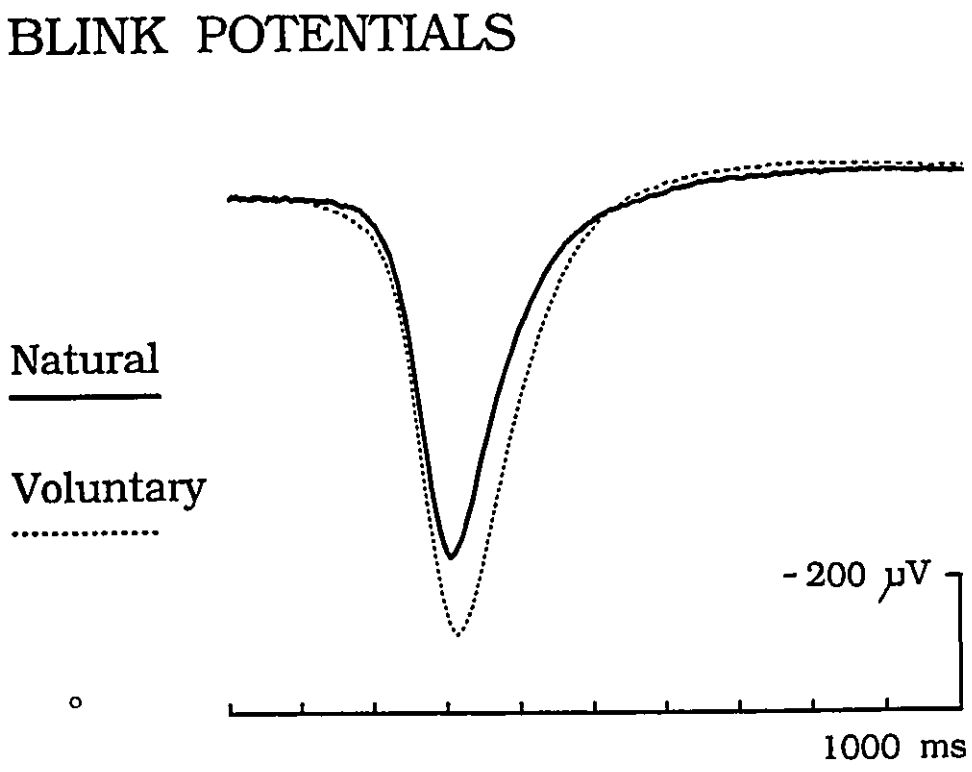

Figure 1: **Natural and voluntary blinks.** These recordings present the average blinks from 12 different subjects. One blink was selected at random from each of the subjects under each of the conditions. The figure demonstrates that the voluntary blink potential is larger in amplitude than the natural blink potential. Furthermore, the time course is different with the mid-portion of a voluntary blink lasting longer.

The measurements of the blink features are presented in Table III.

Table III: Blink parameters.

Measurement	Natural blinks	Voluntary blinks
Duration (ms)		
Total	292±45	287±52
Range (means)	233-355	210-384
Range (values)	125-470	175-495
Onset to peak	109±29	107±17
Peak to end	183±35	181±40
Half amplitude	113±21	133±19*
Amplitude (μV)		
VEOG	399±111	480±144*
Range (means)	192-569	212-755
Range (values)	131-890	78-914
Fp2	214±70	261±93*
Fz	82±27	100±36*
Cz	36±12	44±16*

* Significant difference between natural and voluntary blinks ($p < 0.05$)

No significant correlation was found between blink parameters and head measurements. Onset-to-peak duration was significantly shorter than peak-to-end duration for both natural and voluntary blinks. Voluntary blinks had a significantly larger half-amplitude duration than natural blinks. Voluntary blinks had a significantly larger peak amplitude than natural blinks. There were no significant differences in amplitude between female (494 μV) and male (418 μV) subjects.

Figure 2 shows the intrasubject and intersubject variability of blinks.

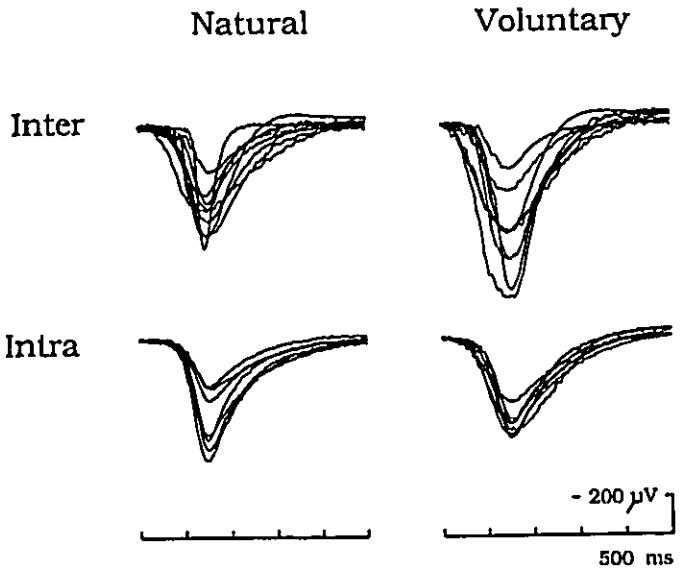

Figure 2. This figure shows blink potentials from 10 different subjects. Nine of the waveforms from nine of the subjects are superimposed in the upper half of the figure to demonstrate the inter-subject variability. These blinks were randomly selected from those available for each subject. The bottom half of the figure shows seven superimposed waveforms for one single subject (not represented in the upper half). This demonstrates the intra-subject variability.

For any one subject, the amplitude of a blink potential varied from blink to blink between about 50 and 150 % (±2 SD) of the mean amplitude.

The rate of change of the potentials (slope) was significantly larger for the onset of voluntary blinks than for the onset of natural blinks (5.7±2.2 vs 4.6±1.8 μV/ms) when measured in the VEOG recording. There were no differences in the offset slopes of the two kinds of blinks (3.8±1.8 μV/ms). The onset slope of the up-saccade potentials was smaller than that of the blinks (when measured over homologous times since the saccade movement did not last as long as the blink-onset) but this difference was not significant.

The rate of change of the slope of the blink potential measured at the peak of a blink (±50ms) was 10.6±4.8 $\mu V/ms^2$ for natural blinks and 9.8±5.0 $\mu V/ms^2$ for voluntary blinks.

Figure 3 illustrates the scalp distribution of blink potentials. These data were obtained by averaging voluntary blinks from one of the subjects at several scalp and face locations. A large positive wave is recorded from the supraorbital ridge together with a small negative wave below the eyes that was about one quarter the amplitude of the supra-orbital wave. In the 8 subjects who participated in the third experiment, the ratio of the potentials recorded on the vertical EOG channel (between the supraorbital and infraorbital ridges) to the potential recorded between the supraorbital ridge and the noncephalic reference was measured: 1.27±0.06.

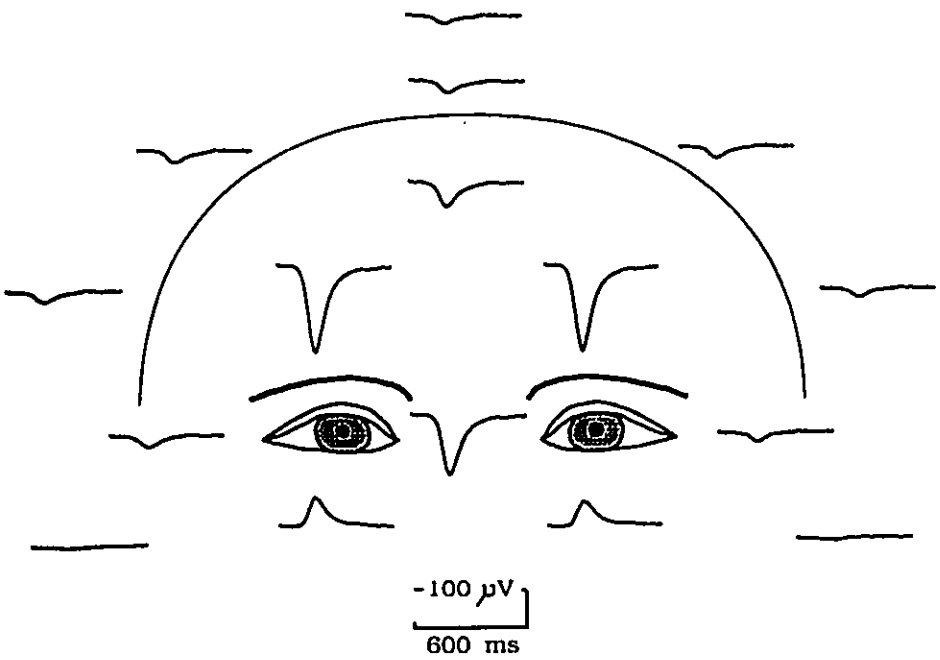

Figure 3: This figure represents the average blinks of 60 voluntary blink potentials from a single subject. Recordings were made from seven electrodes near the eyes and nine scalp locations, relative to a noncephalic reference. The scalp locations were a chain of electrodes going from the left mastoid to the vertex to the right mastoid (M1, T3, C3, Cz, C4, T4, N2) and some additional midsagital electrodes (Pz, Fz).

The blink propagation factors for all scalp locations are presented in Table IV. This table also includes data from the third experiment and from the auditory evoked potential experiment.

Table IV: Vertical propagation factors represent the percentage of the vertical EOG (recorded between the upper and lower orbital ridges) present at each electrode site (referred to a noncephalic reference).
1 - Second Experiment, factors calculated by regressions
2 - Third Experiment, factors calculated by regressions
3 - Third Experiment, factors derived from the source components
4 - Auditory evoked potential experiment

Location	Blinks				Saccades			
	1	2	3	4	1	2	3	4
Fp1/2	47±8				45±11			
Fz	18±5	19±2	19±2	17±9	18±4	22±5	22±3	21±5
F3/4	18±4				19±5			
F5/6				16±6				17±5
F7/8	17±4				15±5			
Cz	8±4	10±3	9±1	8±6	10±4	17±8	15±3	16±6
C3/4	8±3	8±3	9±1	8±5	10±4	11±6	13±3	13±4
T3/4	5±2	7±3	6±2	5±5	6±3	8±5	7±3	7±4
M1/2				2±4				2±4
A1/2	1±1	2±2	1±2		1±2	5±3	2±2	
Pz	5±2	5±3	5±2	6±5	8±6	11±4	13±5	11±6
P3/4	5±2				7±5			
P5/6				5±4				9±5
T5/6	4±2				5±4			
Oz	4±3			4±4	5±4			7±5
O1/2	3±2				5±4			

No significant differences in the propagation factors were found between natural and voluntary blinks at any position. In general there were no differences between homologous electrode locations. However, the Fp1 location showed a significantly larger propagation factor than Fp2. Several factors may have contributed to this unexpected finding. One possibility was that coherent EEG and muscle activity between the upper VEOG and the frontopolar electrodes may have contributed to the calculation of the propagation factors and, because of the shorter distance, this effect would have been

larger for Fp1 than for Fp2. To test for this possibility, blinks were averaged (to decrease the EEG and muscle activity) and the propagation factors were recalculated. The frontopolar left-right difference persisted. Since the EEG and muscle activity would have a higher frequency content than the blink potentials, the signals were also filtered prior to calculating the factors. The blink propagation factor was relatively unaffected by low-pass filtering down to 5 Hz. Furthermore, this filtering did not affect the Fp1-Fp2 difference in the propagation factors. Another possibility was that the placement of the upper VEOG electrode may have decreased the resistance between the upper VEOG electrode and the Fp1 electrode because of spread of the electrolytic paste or because of skin hydration. In 2 subjects who had shown an asymmetrical Fp1 propagation factor in the initial recordings, recordings were conducted using simultaneous left and right eye VEOG montages. There was no clear asymmetry between Fp1 and Fp2 regardless of which EOG channel was used to calculate the propagation factors. In 4 subjects the VEOG was recorded from the left eye on one day and from the right eye on another day. The propagation factor for the frontopolar electrode on the side of the VEOG recording was consistently larger than for the other frontopolar electrode. When using the left eye the average propagation factors were 0.52 for Fp1 and 0.48 for Fp2. When using the right eye the factors were 0.52 and 0.56.

Saccades

Waveforms of sample 20° saccades recorded at the EOG electrodes and several head positions in one subject in the second experiment are presented in Figure 6. The average propagation factors are shown in Tables IV and V together with data from the other experiments. The amplitudes of the saccades in the vertical and horizontal EOG and several scalp electrodes are tabulated in Table VI.

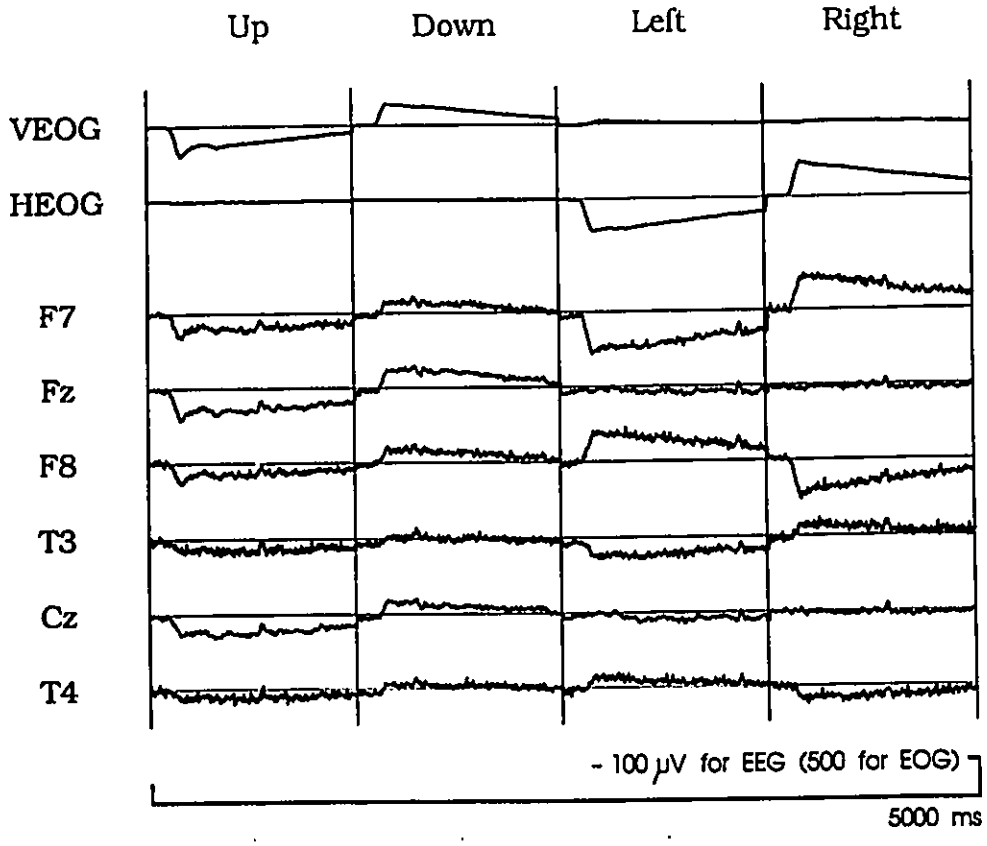

Figure 4. This figure has spliced together the initial portion of an unaveraged 20° saccade-recording in each of the four different directions. The upper two tracings represent the differential EOG recordings and the next six tracings show the EEG recorded (using a noncephalic reference) from different scalp locations. A small EKG artifact can be seen in the EEG recordings.

There was no significant correlation between saccade amplitudes (measured on the EOG channels) and head measurements. Although female subjects had larger horizontal saccade amplitudes than males (males 287±101 μV; females 348±98), this difference was not significant. Vertical saccade amplitudes were almost identical in both sexes (males 237±38; females 233±93).

Table V: Horizontal propagation factors represent the percentage of the HEOG (recorded between electrodes at the external canthi) present in the recordings at each electrode site (referred to a noncephalic reference). The propagation factors at the electrodes away from the midline are unsigned. When the HEOG is recorded between the left external canthus and the right, these factors are positive for the left-sided electrodes and negative for the right.

1 - Second Experiment, factors calculated by regressions.

2 - Third Experiment, factors calculated by regressions

3 - Third Experiment, factors derived from the source components

4 - Auditory evoked potential experiment

Location	Propagation Factors					
	Horizontal Saccades				Reading	Pursuit
	1	2	3	4		
Fp1/2	5±9				8±7	7±11
Fz	0±5	1±5	0±2	-1±5	0±4	0±3
F3/4	8±5				8±4	7±2
F5/6				14±5		
F7/8	22±7				18±8	21±4
Cz	0±5	0±6	0±2	1±3	0±4	0±3
C3/4	4±5	4±6	4±3	5±3	2±4	4±3
T3/4	8±5	5±7	7±6	7±4	6±4	5±4
M1/2				3±3		
O1/2	4±5	3±3	3±3		4±4	2±3
Pz	1±4	2±5	1±2	1±4	-1±6	1±2
P3/4	2±4				1±2	1±2
P5/6				3±4		
T5/6	3±4				2±3	1±2
Oz	0±3			0±3	-1±4	0±2
O1/2	1±3				1±3	0±1

Up-saccades were not significantly different in amplitude from down-saccades and left-saccades were not significantly different from right-saccades. However, as shown in Table VI, horizontal saccades (measured on the HEOG channel) had significantly larger amplitudes than vertical saccades (measured on the VEOG channel).

As shown in Table VI, the EOG amplitude increased for the larger movements in the same proportion at all electrode sites. The conversion factors were 12 μV/° for the VEOG and 16 μV/° for the horizontal EOG. Using these factors, we could accurately predict the amplitudes of the diagonal saccades on the VEOG and HEOG channels.

Table VI: Saccade amplitudes (μV)

	10°	20°
Vertical saccades		
VEOG	118±37	230±75
Fp1 / 2	55±17	99±10)
F3 / 4	22±7	44±5
C3 / 4	11±3	23±4
Horizontal saccades		
HEOG	164±50	323±100
F7 / 8	35±11	71±7
T3 / 4	14±4	29±6

The durations of the saccades (from onset to peak) did not vary with the direction of the saccade. However, the 20° saccades took significantly longer (80±16 ms) than the 10° saccades (54±14 ms).

As illustrated in Figure 5 the distribution of the up-saccade potential over the face and scalp is quite different from that of a blink. The saccade is recorded with almost equal amplitude below the eye as above whereas the blink is much larger above the eye. Furthermore, the up-saccade spreads further back on the scalp than a blink.

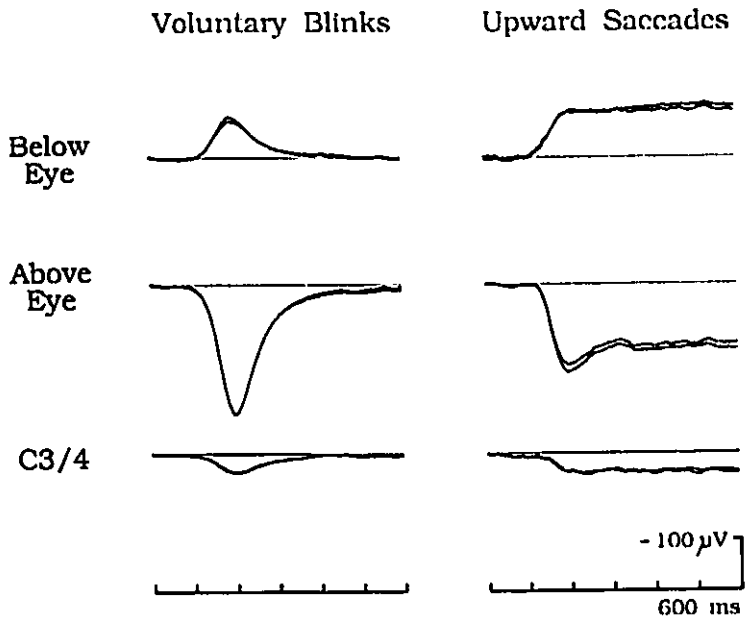

Figure 5: Blinks and vertical saccades. This figure presents the average recording of blinks and vertical saccades from a single subject. The figure demonstrates that the potentials recorded during saccade are approximately equal (and of opposite polarity) below the eye and above the eye, whereas the blink potentials are much smaller below the eye. Furthermore, although the blink potentials near the eye are larger, the spread of the potential to posterior areas of the scalp is less and the amplitude of the potential recorded at the vertex is approximately equal for the blinks and the saccade.

In ten of the twelve (83%) subjects in the second experiment, the initial 100 ms of the vertical EOG for the up-saccades was significantly distorted by a superimposed positive wave. These additional potentials can be seen in Figure 4 and Figure 5 and are identified as "rider" artifacts in Figure 6. These artifacts made it very difficult to distinguish blinks from up-saccades on the basis of the rate of change of the slope of the potential unless these values were assessed over more than 150 ms after the peak.

If the change in the potential over the 50 ms prior to the peak is added to the (negated) change over the 200 ms after the peak, a value of 300 μV would successfully distinguish between all of the blinks (>300) and all of the saccades (<300) recorded from the 12 subjects (based on average blink and 20° saccade values for each subject).

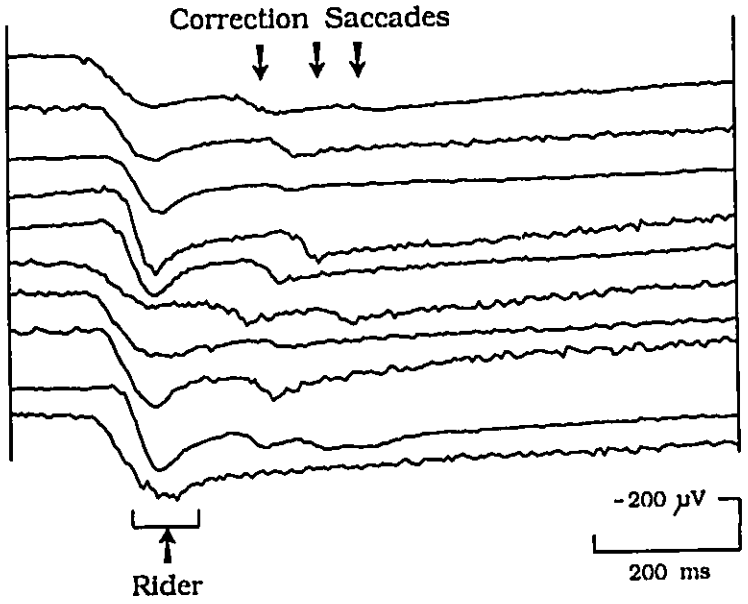

Figure 6: Up-saccade. This figure represents the initial portion of the potentials related to 20° up-saccades from ten different subjects. The recordings were obtained from the bipolar VEOG channel. The figure demonstrates a "rider" potential riding on top of the initial portion of the potential in seven of the ten subjects. As well, there are correction saccades occurring between 150-250 ms after the end of the initial saccade.

In approximately 80% of the 20° saccades there were small additional deflections that began between 150 and 250 ms after the end of the initial saccade deflection. These probably represented "correction saccades" (Becker and Fuchs 1969) and are identified as such in Figure 8. These events occurred in all saccade directions. They were also present in the 10° saccades but they were much less frequent (about 30%) and much smaller (and therefore very difficult to recognize).

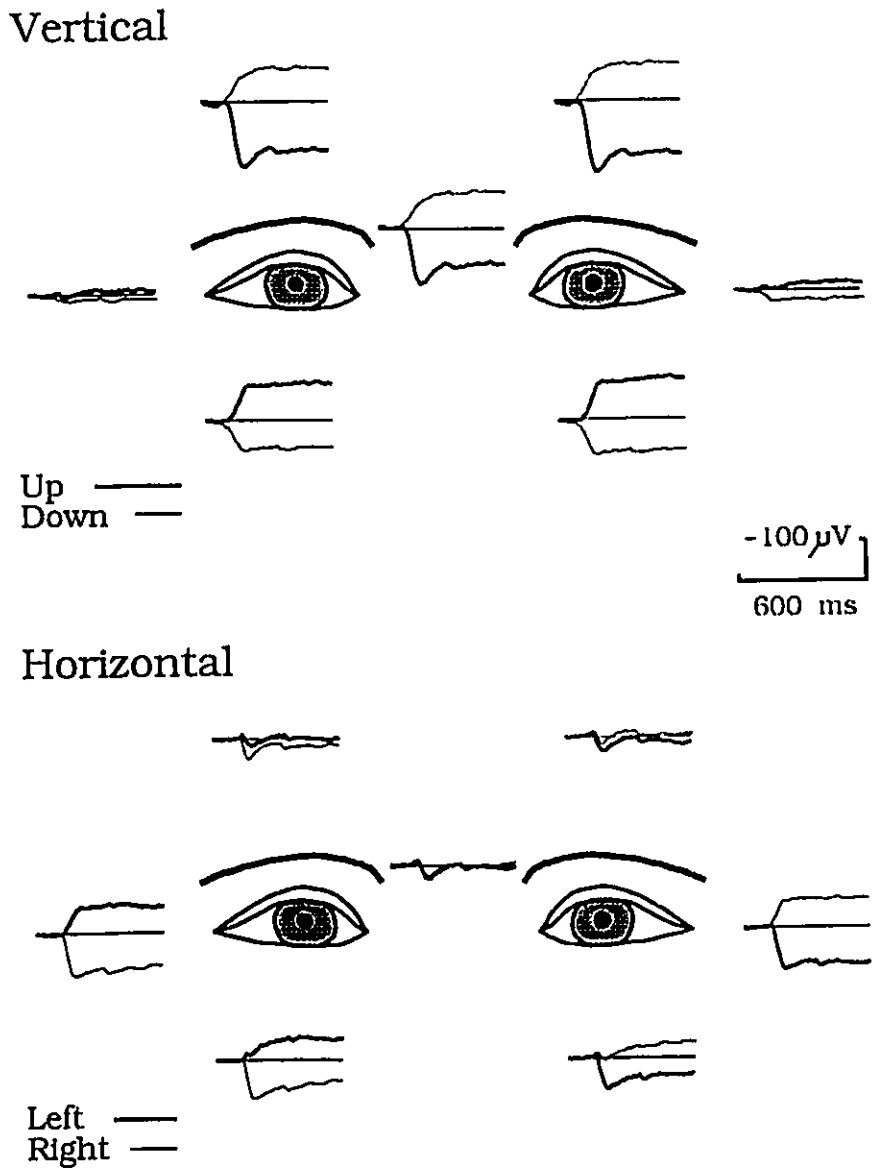

Figure 7: **Vertical and horizontal saccades.** This figure shows recordings between the peri-ocular electrodes and the noncephalic reference. Each tracing represents the average of ten saccades from one subject in the third experiment. The upper half of the figure shows the vertical saccades. The potentials recorded above the eye are somewhat greater than those recorded below the eye, particularly for the up-saccades. Furthermore, the potentials recorded for the down-saccades are smaller than those recorded for up-saccades. The up-saccade shows a clear "rider" artifact in the initial portion of the recording. In the lower half of the figure the potentials associated with horizontal saccades are shown. The amplitude of the positive wave on the side toward which the eyes move is greater than the amplitude of the negative wave on the opposite side.

Examination of the recordings from the third experiment, in which the peri-ocular electrodes were referred to the noncephalic electrode, allowed consideration of the relative contributions of the two electrodes in each of the horizontal and vertical EOG recordings.

When looking to one side the positive potential at the lateral canthus on that side was a little larger than the negative potential at the opposite canthus (151 vs 124 μV). The saccade potential recorded between the canthus and the nasion was approximately one half the potential recorded between the two external canthi, with the potential recorded over the eye ipsilateral to the direction of the saccade being a little larger than over the other eye.

For the vertical eye movements, the following differences were noted: the potential recorded above the eye was larger than the potential recorded below the eye regardless of whether the movement was up or down, and this difference was larger for down-saccades. These findings are illustrated in Figure 7.

In seven of the twelve subjects examined in the second experiment, a clear spike potential ranging from 25 to 55 μV (40±6) in amplitude and lasting from 15 to 50 ms (35±9) was seen at the F7 or F8 electrode at the beginning of the lateral eye movements toward that electrode. This is illustrated in Figure 8 which shows a recording taken during reading. Those subjects without a recognizable spike may have had such a potential obscured by background muscle noise. This spike did not show up in the average recordings, probably because the timing from the peak of the saccade varied slightly from subject to subject.

Reading and following eye movements

The reading condition elicited stepwise saccades and the following eye movements were associated with sinusoidal potentials. These are illustrated in Figures 8 and 9.

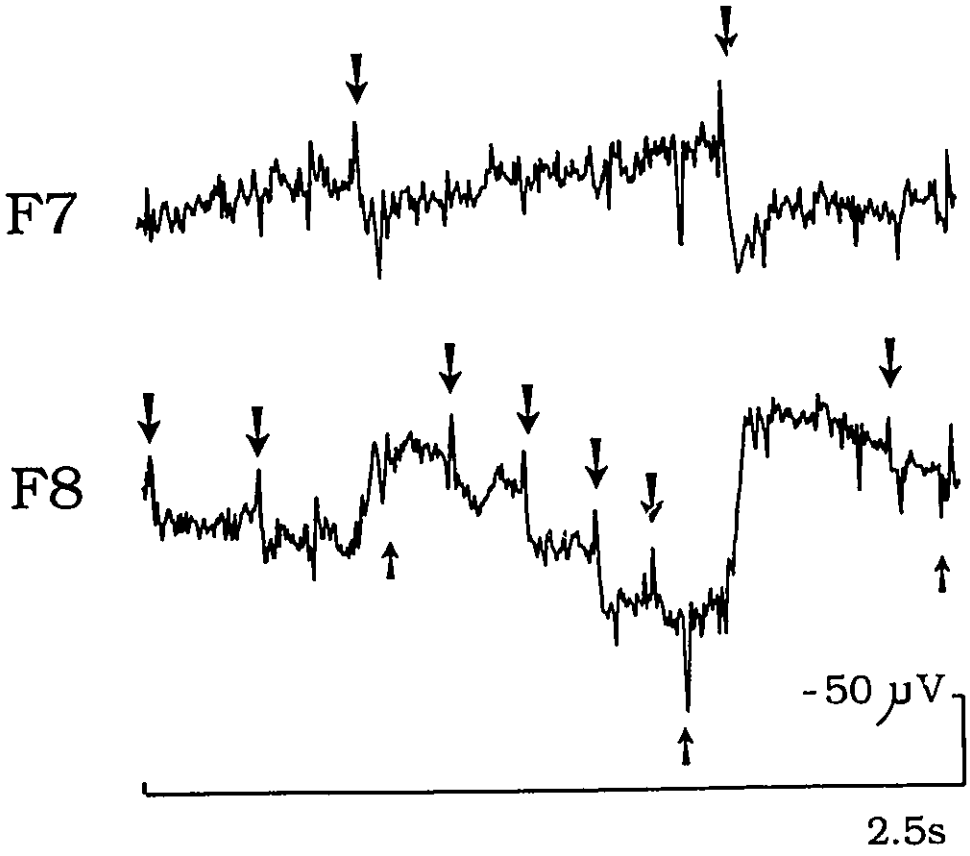

Figure 8: Ocular potentials during reading. This figure shows the potentials recorded from the F7 and F8 electrodes using a noncephalic reference. The general reading pattern consists of a series of between 3 and 5 right saccades followed by a large left saccade as the eyes move back to the beginning of the next line. At the beginning of each of the right saccades there is a small spike potential recorded at F8 and at the beginning of the left saccade there is a small spike recorded at F7. These "lateral ocular spicules" are indicated by the downward arrows. These inferior frontal electrodes pick up a fair amount of muscle activity throughout the recording. Some of this muscle activity may also be coming from the noncephalic reference. As well, there is some EKG artifact that was not completely balanced out. This is indicated by the upgoing arrows.

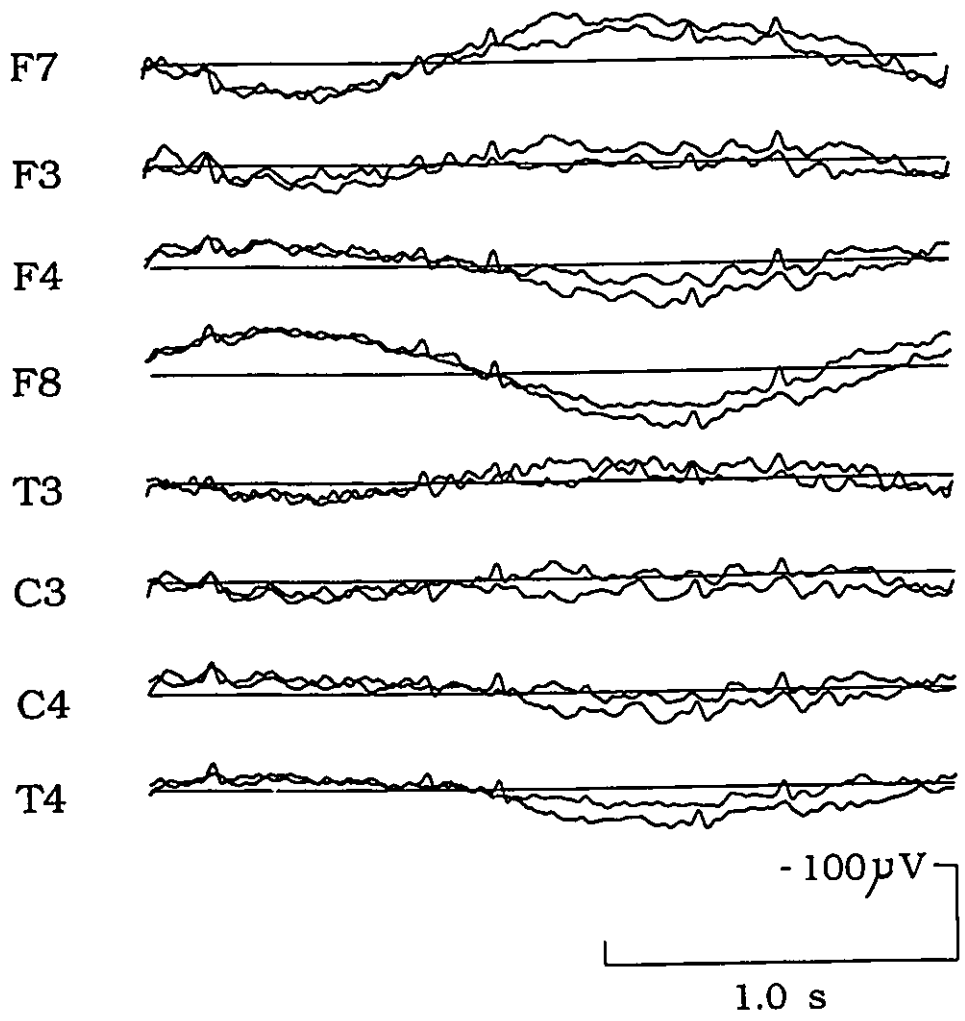

Figure 9: Potentials recorded during following eye movements. These potentials were recorded from a subject as he fixated a tennis ball swinging back and forth between 10 ° on the left and 10 ° on the right at a rate of 1 cycle every 2.5 second. Single recordings from two separate cycles of pursuit by one subject are superimposed.

Propagation factors for vertical eye movements

The vertical propagation factors are shown in Table IV. There was no significant correlation between these factors and any measurement of head size. Vertical propagation factors were larger at Fp1 than at Fp2, but this difference was not significant. There were

no significant differences in the vertical propagation factors of 20° and 10° saccades. The 10° saccade propagation factors were larger at Fp1/2 (47±7 versus 43±10) and F7/8 (16±4 versus 14±5). Recalculating the propagation factors after averaging the saccades removed these differences.

No significant differences in the vertical propagation factors were found between up-saccades and down-saccades in the second experiment. However, measurements on the data from the third experiment, where activity was recorded between the EOG electrodes and a noncephalic reference, revealed that down-saccades had larger amplitudes at the upper VEOG electrode than at the lower VEOG electrode (-170 vs 128 μV). This is illustrated in Figure 9.

Saccade vertical propagation factors had a different scalp distribution from blinks. At the frontopolar electrodes, blink propagation factors were larger than vertical saccades propagation factors, but these differences were not significant. The propagation factors for blinks decreased more rapidly from front to back of the head than those for vertical saccades. At the central, parietal, occipital and posterior-temporal regions, the propagation factors for vertical saccades were significantly larger than those for blinks.

Propagation factors for the 20° up-saccades were calculated with and without the initial rider artifact. There was a tendency for the initial portion of the vertical saccade to have larger factors at the frontopolar electrodes and smaller factors at the posterior electrodes. At Fp1 the factor was 0.40 during the distortion and 0.38 outside the distortion (compared to 0.49 during a blink); at P3 the factors were 0.07, 0.09 and 0.05, respectively. However, the variability was high and the differences were not significant.

The propagation factors obtained in the third experiment were very similar to those seen in the second experiment. In the third experiment, the subjects repeated the different eye movements many more times. This led to boredom and drowsiness which in some subjects, was associated with some widespread theta and alpha activity. Data from multiple single recordings were usually entered independently into the regression analysis and in these drowsy subjects the regression coefficients were larger than expected, probably because the widespread EEG activity was also being picked up at the peri-ocular electrodes. Averaging the recordings for each eye movement prior to entering the data into the regression analysis attenuated the EEG activity and provided more reasonable propagation factors.

Propagation factors for horizontal eye movements

The propagation factors for horizontal eye movements are shown in Table V. Because the left electrode was used as input 1 in the horizontal EOG recordings, the horizontal propagation factors had positive values on the left side of the head and negative values on the right side. The table shows absolute values. Comparisons between the 20° and 10° saccades revealed that the 20° saccade horizontal propagation factors were significantly smaller (in absolute values) than the 10° saccade factors at F7 and F8. Since this difference vanished if the factors were recalculated after low-pass filtering the recordings, the effects can be attributed to the EEG and muscle activity in the temporalis muscles. These activities would have a greater effect on the smaller potentials.

Measurements in the third experiment revealed differences between right and left saccades. Right saccade potentials were larger in amplitude at the electrode by the external canthus of the right eye then left saccades (156 vs -128 μV). Left saccades were larger at the external canthus of the left eye (147 versus -120 μV).

Unlike the potentials associated with blinks and vertical saccades, those associated with horizontal saccades were significantly related to some head measurements. There was a significant negative correlation (r= -0.60) between the T3/4 horizontal propagation factors and the distance between the two preauricular points. The F7/8 propagation factors did not quite reach significance (r= -0.55). Head circumference was also negatively related to the F7/8 and T3/4 horizontal propagation factors (r= -0.54 and -0.51 respectively) although, again, these relationships were not quite significant.

The horizontal propagation factors for the reading and smooth pursuit conditions are also tabulated in Table V. These factors were symmetrical and showed no significant differences from the factors for 20° horizontal saccades.

Variability of the propagation factors among subjects

The variability of the propagation factors among subjects is tabulated in Table VII. Variability increased from the front to the back of the head. Blink propagation factors had smaller variability than saccade propagation factors.

Table VII: Inter-subject variability of propagation factors. Variability is expressed as coefficient of variation (standard deviation × 100 ÷ mean)

		electrode location				
propagation factors	**artifact**	**Fp1/2**	**F3/4**	**C3/4**	**P3/4**	**O1/2**
vertical	blinks	17	22	38	40	67
	saccades	24	26	50	71	80
		F7/8	**T3/4**	**T5/6**	**O1/2**	
horizontal	saccades	27	56	133	300	

DISCUSSION

Corneal potentials

Picton and Hillyard (1972) recorded surface potentials of about -30 mV from the scalp and face relative to subcutaneous tissues. Comparable measurements can be obtained from our data by subtracting the potential at the scratched mastoid from the others. The resultant potentials from the intact forehead, cheek and vertex are smaller than in 1972. The difference may be related to the skin becoming partially hydrated by the fluid in the wick electrode. This was a particular problem at the vertex which was used as a reference in all recordings. The 1972 recordings were obtained using electrode-jelly.

The surface recordings from the cornea relative to the vertex showed no potential difference. When corneal potentials were measured relative to the skin on the forehead or cheek, the cornea was between 10-15 mV more positive. Multiple generators contribute to the corneal recording. The retina and lens generate potential fields that have their positive poles directed toward the cornea. However, like the skin, the outside of the cornea is negative relative to the inside with a transcorneal potential between 15 and 42 mV (Donn et al. 1959) and this will counteract the fields from the retina and lens. Some of the discrepancies in the literature concerning the magnitude of the corneoretinal potential are probably related to the locations of the measuring electrodes. If the potential is measured directly across the retina, the potential is about 30 mV (Lasansky and de Fisch 1966); if measured between the cornea and the fundus (or optic nerve) the potential is of the order of 5 mV (Granit 1947). At a short distance away from the eyes the potential is about 1 mV. This can be estimated by recording the field changes when the eyes rotate. A 60° rotation would result in an equivalent dipole equal in magnitude to the resting dipole. (This might be more easily visualized if one consults Figure 16 of Chapter 2). If

the eyes move from 30° in one direction to 30° in the opposite direction, the change in potential measured about 1 cm from the eye is between 0.5 and 1.0 mV. Furthermore, during a blink when the eyelid covers the cornea and connects the positive pole of the corneofundal dipole to the adjacent skin the potential recorded there increases by about 0.5 mV.

Technical Aspects of Calculating Propagation Factors

Propagation factors are usually calculated by measuring the ratio of the recording during an eye movement at a particular location to that obtained from the ocular monitoring electrodes. A difficult problem arises if this calculation is performed on raw recordings. As well as the EOG, other signals may also be picked up simultaneously in the two recordings, EEG and muscle being the most common. These signals will have a different scalp distribution from the EOG and will significantly distort the calculation of the propagation factors. These problems may be particularly evident when the muscle levels are high or when widespread EEG rhythms occur during drowsiness. These problems can be attenuated in two ways. First, the multiple recordings can be averaged after time-locking to the peak of the blink (Semlitsch at al. 1986) or the saccade. Second, the recordings can be filtered so that the EEG and muscle activity are selectively attenuated. In the present investigation, a high-pass filter setting of 5 Hz removed most of the muscle activity while not significantly affecting the EOG signals. A final technical caveat is that propagation factors should not be calculated using an EOG recording referred to the same electrode as the EEG signal. The signals picked up from the common reference may significantly distort the propagation factors. The usual approach, therefore, is to record the EOG signals using a differential recording from electrodes on either side of the eye. Another approach would be to use an average reference when calculating the factors.

Some unexpected asymmetries were observed in the vertical propagation factors at the frontopolar electrodes. The blink propagation factor was larger at Fp1 than at Fp2 when the VEOG was monitored from above and below the left eye. Vertical saccade factors were also larger at Fp1 than at Fp2 but this difference was not significant, probably because of the larger variability of the saccade factors. This asymmetry was most probably due to some partial short-circuit between Fp1 and the upper VEOG electrode caused by the electrode paste or skin hydration. This would make the Fp1 electrode pick up larger ocular potentials than it should. This explains why the asymmetry was diminished when bilateral VEOG recordings were made (both Fp1 and Fp2 would be short-circuited) and why the asymmetry was reversed when a unilateral VEOG recording over the right eye was conducted.

Blinks

The blink durations we measured from the electrical recordings are longer than those obtained from cinematographic studies (Doane 1980). In that report the mean duration of the closing phase for the upper eyelid was 82 ms whereas in the present study the onset-to-peak duration of the electrical change was 108 ms. These discrepancies may be related to differences between the subjects in the two studies since some of the recordings illustrated in the Doane paper show durations very similar to ours. The electrical measurements may also pick up the beginning of the movement somewhat earlier than the cinematographic measurements. Furthermore, some blinks are faster than others and Doane states that the data in his tables are representative of a "standard fast blink". The present results agree with Doane's finding that the opening phase is longer than the closing phase -- Doane's results give a ratio of 2.1 : 1 and ours a ratio of 1.7 : 1. Doane also observed that natural blinks differ from those of a voluntary nature in that they often have a lesser excursion, with only 25% going to complete closure, and a longer stationary

period between the closing and opening phases (30 ms as opposed to 4 ms). Data from the present study shows that voluntary blinks have larger amplitudes than natural blinks. Also, voluntary blink potentials have a different waveform relative to natural blinks, with a similar total duration but a larger duration at the middle of the blink. The eyelid moves faster in voluntary blinks than in natural blinks and there is a brief pause between the closing and opening movements in the voluntary blink that is not present in the natural blink.

Saccades

The amplitude of the saccade potentials depends on the angular magnitude of the saccade, the position of the recording electrodes, and the amplitude of the corneofundal potential. By standardizing the magnitude of the saccade and the position of the electrodes, the electrooculogram can be used as a non-invasive method of indirectly measuring the corneofundal potential. Average measurements of the horizontal EOG in this study - 16 μV/° - are comparable to those of Krogh (1975, 1976) who reported median baseline measurements of 368 μV for a 30° movement (12 μV/°) provided differences in the recording conditions are considered. Krogh recorded with electrodes placed at the sides of each eye while we used electrodes placed at the external canthi of both eyes. The potential difference between the external canthus of an eye and the nasion is about a half of that measured between the external canthi of the two eyes. Furthermore, Krogh recorded after dark adaptation whereas in this study the recordings were in normal room lighting. Krogh used DC recording techniques whereas in this study a 1-s time constant (low frequency cutoff of 0.15 Hz) was used.

Significant sex differences have been described for the corneofundal potentials (Krogh 1976). In this study the potentials were slightly larger in females than in males,

but this difference was not significant. Non-significant differences were also found between head size, with males having heads slightly larger than females. Head size differences might contribute to the differences in corneofundal potentials found in this and others studies. As the corneofundal potential is affected by such factors as metabolic state, it is also possible that metabolic differences related to sex might play a role in these differences.

Differences between Blinks and Saccades

The scalp-distributions of the potentials associated with vertical saccades and blinks were clearly different. Blinks have fields that are larger at the frontopolar electrodes and decrease more rapidly from the front to the back of the head. The results in Tables 4 and 5 agree with those reported previously for some electrodes in other studies. In the papers reviewed by Elbert et al. (1985), the propagation factor for the vertex electrode averaged 14 (range 9-19) for vertical saccades compared to 8 (range 7-9) for blinks. The estimated size of a vertical eye-movement (12 μV/°) necessary to explain the recorded magnitude of a blink (400 μV) would be over 30°. This would be highly unlikely - the normal movement of the eye during prolonged closure is at most 20° (Collewijn et al. 1985).

Upward eye movements show a positivity at the frontal pole and an approximately equal negativity at the cheek, whereas blink potentials are quite asymmetrical with a smaller negativity at the cheek (Figure 5). The rotation of one eye generates similar fields of opposite polarity above and below the eye, whereas the sliding of the upper lid generates a larger field above than below the eye (Antervo at al. 1985). The reason for the negativity at the cheek is not immediately clear. It is caused by the location of the reference for the recordings (the noncephalic electrode) and some decreased flow of

current in the cheek region compared to the forehead. The increased current flow during a blink is oriented radially and slightly upward (Antervo at al. 1985). The electrode montage between the forehead and the reference records directly across this current dipole, whereas the montage between the cheek and the reference records diagonally with the cheek electrode located just below the midpoint of the dipole.

Different mechanisms must therefore generate the potentials associated with blinks and saccades. The present results support the "sliding electrode" hypothesis first proposed by Matsuo at al. (1975) -- the eyelid moving down the cornea connects the front of the head to the positively charged anterior pole of the eyes. This is quite different from the effects of an upward eye movement ("Bell's phenomenon" hypothesis).

Barry and Jones (1965) showed that the distortion that occurs at the onset of up-saccades is most probably caused by the eyelid. In the present study the propagation factors during the "rider artifact" have values between those of the blinks and the later part of the saccade. This suggests that a similar mechanism generates blinks and the "rider artifacts". This topic will be investigated in the next chapter.

3

SOURCE DIPOLES AND SOURCE COMPONENTS

INTRODUCTION

The EEG is a very complex recording. Event-related potentials are somewhat easier to evaluate since they are specifically tied to some event, but they are also very complex. The main problem is that many different generators contribute to scalp-recorded waveforms. Topographical mapping of these potentials may make multiple waveforms easier to interpret. However, prominent peaks or troughs in the scalp-recorded waveforms do not necessarily correspond to the activity of a single generator (Näätänen and Picton 1987) and do not necessarily indicate periods of maximal or minimal activity in these generators (Picton 1990).

Brain Electric Source Analysis (BESA) and Principal Components Analysis (PCA) are tools that can be used to study the generators (or sources) that underlies the scalp-recorded waveforms. BESA starts from a given source configuration, calculates the scalp-distribution of the fields resulting from these sources (using a mathematical head model), compares the calculated scalp-distribution with the recorded data, and then iteractively changes the source configuration to minimize the difference between the modeled waveforms and the recorded data. The solution will be the source configuration generating the scalp-potentials that most closely fit the recorded data. The sources are expressed as dipoles. The electrical activities of the sources are represented by changes in the dipole strength over time. The use of PCA for analyzing scalp-recorded waveforms is

based on a similar idea: that the scalp-recorded waveforms are a linear superposition of basic source waveforms. PCA decomposes a set of variables into orthogonal components. The components are thought to represent the processes responsible for the correlation among the variables. PCA calculates this basic set of waveforms differently than BESA. One difference is that PCA does not use head models. BESA is, thus, a more "physiological" approach than PCA. However, this feature of PCA may become useful for correction of ocular artifacts.

BESA and PCA may increase our understanding of the different processes that contribute to the ocular artifacts since they probably derive from several generator processes. Although some authors attribute blink potentials to the occurrence of a vertical eye movement (Bell's phenomenon) during the blink, others attribute these potentials to the eyelid acting as a sliding electrode connecting the forehead to the positively charged cornea. The rider artifact, a distortion of the EOG that occurs at the onset of upward saccades, may not due to saccade-overshoot but to the eye moving briefly under the eyelid at the onset of an upward saccade.

Source dipoles and source components may also be helpful in removing ocular artifacts from the EEG and the event-related potentials. As seen in the previous chapter, even if one recognizes that blinks and saccades need to be compensated differently, it may be difficult to differentiate between them, particularly if they occur together (as in the rider artifact). BESA and PCA may provide objective ways to remove these overlapping processes from the EEG.

In this chapter we present the results of our studies of the ocular artifacts using BESA and PCA.

METHODS

Recordings

These studies used data from the third experiment described in Chapter 2. The locations of the electrodes used in this experiment are shown in Figure 10. Both the EOG and EEG electrodes were referred to the noncephalic reference.

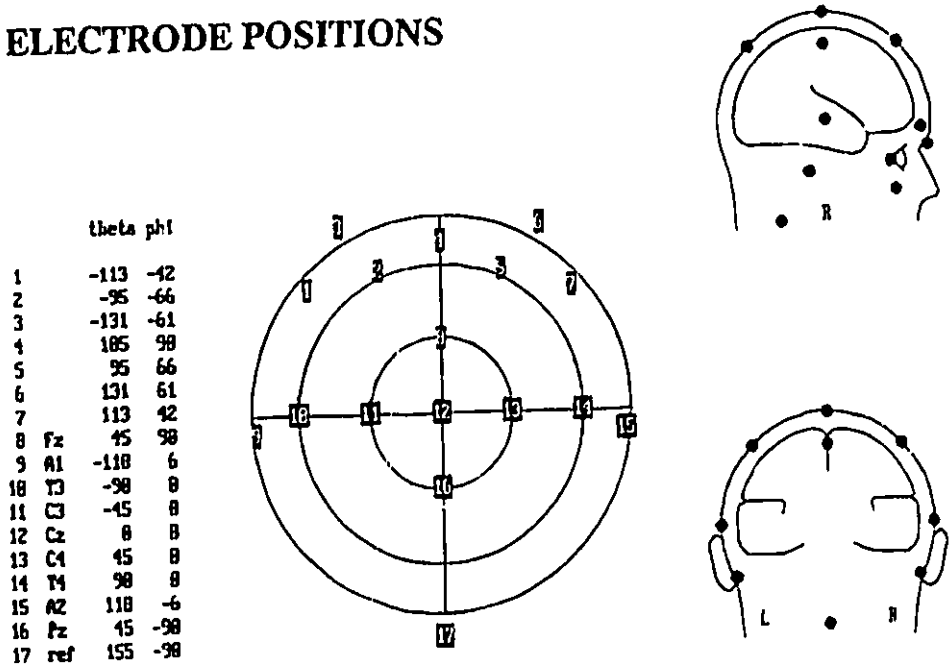

Figure 10: Electrode locations. This figure shows the locations of the different recording electrodes used in the third experiment. The first seven electrodes were located near the eyes. Electrodes 8-16 were located on the scalp. All electrodes were referred to a balanced noncephalic reference (17). In the center of the figure the locations are plotted on a view of the head that looks down on the vertex. This uses an azimuthal equidistant projection, which allows one to plot points that are below the "equator" (theta=0°). The outer circle represents the level of the ear lobes. The left side of the figure shows the coordinates of the seventeen electrodes. The right side of the figure shows the locations of the electrodes on a lateral and a frontal view of the head.

Averaging and combining recordings

Average blinks were obtained by time-locking to the peak of the blink-potential and averaging the data recorded up to 200 ms before and up to 400 ms after the peak. For saccades, averaging was time-locked to the peak of the saccade and the same latency-ranges were used. The ten examples of each particular eye movement (blinks and the four different saccades) from each subject were averaged together to give relatively noise-free waveforms. Different recordings were combined into single tracings. Before splicing the traces together the baselines were adjusted to the initial 50 ms of each trace and low-pass filtered at 15 Hz (24 dB/octave slope). The average recordings were also spliced together to make two other combined recordings, the up and down saccades and the left and right saccades. Prior to analysis the data were collapsed down to fewer points (a 6 ms address time rather than 5 ms) using a spline interpolation.

Dipole source analysis

Dipole source analysis was performed using the BESA programs (Scherg 1990). Source analysis was performed separately for blinks and for each of the saccades (up, down, left, right). The blink solutions were obtained for two sources, with a fitting criterion based solely on minimizing the residual variance over the period from 100 ms before the peak of the blink to 150 ms after the peak. The initial eye-movement solutions ("up-2", "down-2", etc.) were obtained by fitting two dipoles during the stable phase 150-400 ms after the peak of the saccade. For each direction a four-dipole solution ("up-4", "down-4", etc.) was obtained by adding two more sources to fit the rider potentials in the period from the beginning of the saccade to 150 ms after the peak. These extra dipoles turned out to be almost identical to the blink dipoles. The up and down saccades were

modeled by combining the up-2, down-2 and blink solutions to determine the relative contributions of each source to the different recordings. Finally, the data set that combined blinks and saccades in 4 different directions was modelled using six independent dipoles. This model ("all-6") used three pairs of dipoles (one in each eye) to fit the vertical eye-movements, the horizontal eye-movements and the blinks over their respective epochs. The two dipoles from the blink solution were combined with the 2 dipoles from the up-2 solution. We then added the dipoles of abducting eye from each of the left-2 and right-2 solutions. Each of the three pairs of dipoles was fitted during their respective epoch (blink, vertical saccades and horizontal saccades). Only the dipole pair that was maximally active during each of the three epochs was switched on during the fitting.

The locations of the *dipole sources* were described in terms of three parameters: the eccentricity (the distance from the center of the head model to the source expressed as a ratio of the 8.5 cm radius of the three shell model used in BESA); the azimuth or theta (the angle formed with the vertical axis by the line joining the source location to the center of the head); and the longitude or phi (the angle formed with the coronal plane by the line joining the source location to the center of the head). The orientations of the dipoles were expressed in terms of theta and phi. The sign-convention for theta is that left-sided locations have negative values and right-sided locations positive values. For phi, the angle is positive as it rotates anticlockwise from the coronal plane. The strength of the dipole as a function of time is given by the dipole source potentials. The dipole strength was measured in "effective μV". This is an arbitrary unit that describes the strength of a dipole independent of its distance from the surface. A tangential dipole of 0.6 μVeff located at an eccentricity of 60% with a longitude (phi) of 90 would produce a voltage difference of 1 μV between C3 and C4 (Scherg and von Cramon 1986).

A general understanding of these conventions can be obtained from Figure 10 which shows the electrode locations in the third experiment in terms of theta and phi, and from Figure 11 which shows the six parameters of a dipole source.

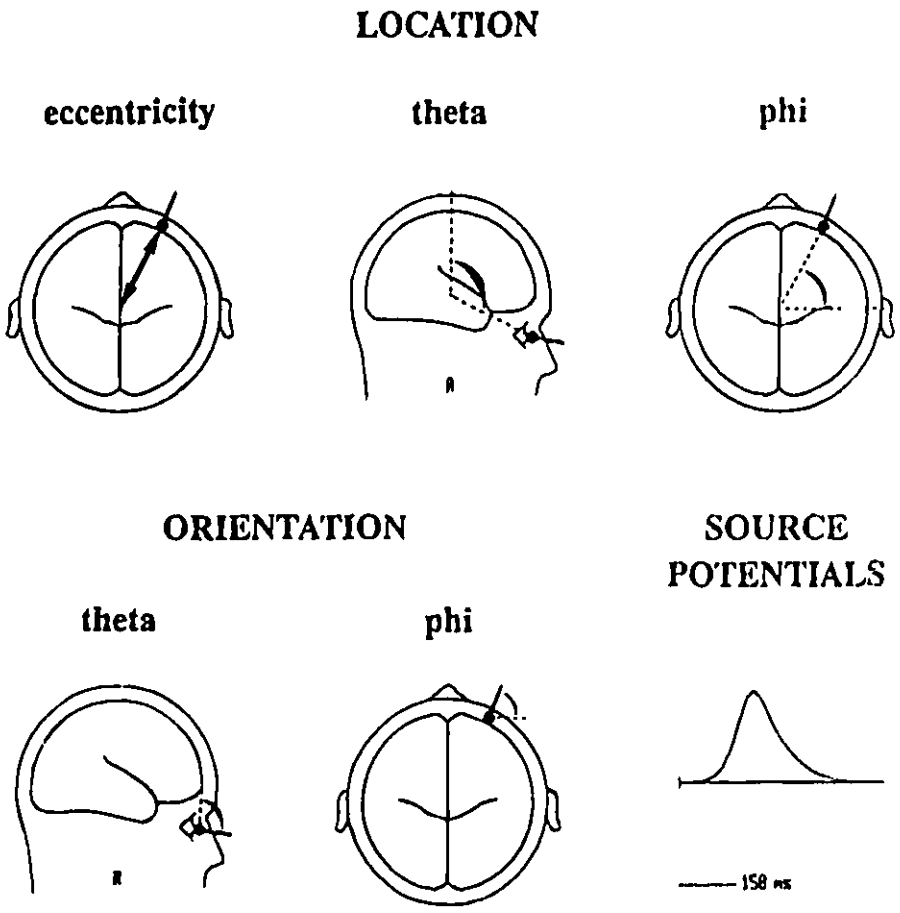

Figure 11: **Source parameters.** This figure illustrates how BESA describes modeled sources. For simplicity, only one dipole is shown (a blink dipole). A source dipole is defined by its location, orientation and strength. **Location** is expressed by 3 parameters: eccentricity, azimuth (theta) and longitude (phi). *Eccentricity* is the distance from the source to the center of the head model. It is expressed as a percentage of the 8.5 cm radius of the three shell head model used in BESA. *Theta* is the angle formed with the vertical axis by the line joining the source location to the center of the head. *Phi* is the angle formed with the coronal plane by a line joining the source and the center of the head. **Orientation** is expressed by 2 parameters: theta and phi. These are measured using the same references as the angles used to express location. The sign-convention for theta is that a positive sign indicates right-sided location or right-going orientation and a negative sign indicates left-sided location or left-going orientation. For phi, a negative sign means clockwise rotation and a positive sign means anti-clockwise rotation from the coronal plane. The strength of the dipole as a function of time is given by the dipole source potentials.

Principal component analysis

The *ocular source components* were estimated using routines available in version 1.9 of the BESA programs (Berg and Scherg 1991b; Berg et al. 1992). A PCA was performed on the data recorded during the eye movements. The average and combined recordings were used for these analyses. A PCA of these data sets provided a set of source components. The weighting factors of each of these source components at the different electrodes could then be used in conjunction with the dipoles used in the forward solution of the EEG sources. Two different techniques were used to assess the source components and weighting functions. The first approach ("PCA-1") was to perform a PCA of the combined data set from all the different eye movements. The first five components of this analysis were chosen to provide a set of EOG source components (in preliminary studies just the first three components were used). In the second approach ("PCA-3"), the blinks, the vertical eye movements and the horizontal movements were analyzed separately, i.e., three different PCAs were performed. The first component (explaining most of the recorded variance) for the blink and the first two components of each of the vertical and horizontal eye-movements, were than chosen and these five components were combined into one set of VEOG coefficients.

Plotting conventions

The scalp-recorded data are plotted negative up since this is the convention for EEG recordings. The waveforms showing the time-course of activity in the dipole source and source components are plotted positive up.

RESULTS

Source dipoles

Single dipole solutions for the blinks and the four different eye movements (20° saccades) were located on the parasagittal plane between the eyes. These solutions did not fit the recorded data very well, leaving 20 to 45% of the variance unexplained. Solutions involving two dipoles (one for each eye) were far more effective in fitting the recorded data. Four-dipole models for the horizontal and vertical eye movements were also obtained. The numerical parameters of the solutions are shown in Table VIII.

Table VIII: Source dipoles for the EOG. Only the right eye dipoles are shown. The left eye dipoles were symmetrical in both position and orientation to the right eye dipoles except for the horizontal saccades. The left eye dipoles for left-saccades were symmetrical to the right eye dipoles for right saccades, and the left eye dipoles for right-saccades were symmetrical to the right eye dipoles for left-saccades.
Since the 4-dipole solutions for the saccades have the same initial pair of dipoles as the 2-dipole solutions, only the third (or fourth) dipoles are tabulated.
Eccentricity is expressed as a percentage of the radius of the head model.
Theta and Phi angles for the locations and orientations are in degrees.
Residual Variance (RV) is calculated over 350 ms for the blink dipoles and over 600 ms for the saccades. This is the percentage of the recorded variance unexplained by the dipole model

EOG	Sources					RV
	Location			Orientation		
	Ecc	Theta	Phi	Theta	Phi	
Blink-2	100±0	114±1	63±2	100±1	68±2	0.3±0.1
Up-2	97±4	112±4	68±5	-14±13	-45±44	2.3±1.4
Up-4	99±2	116±5	68±5	101±1	71±4	0.4±0.1
Down-2	100±0	109±2	76±2	166±12	-38±29	1.2±0.9
Down-4	97±2	114±5	72±10	112±9	69±9	0.4±0.2
Left-2	100±0	114±5	65±2	-96±5	-13±6	1.3±0.5
Left-4	96±2	112±6	65±4	107±8	67±9	0.9±0.3
Right-2	99±1	112±6	64±1	91±8	-5±10	1.1±0.5
Right-4	96±2	116±6	57±3	106±4	71±6	0.7±0.2

All two-dipole solutions placed dipoles on the surface of the head model at an azimuth of about 112 degrees and a longitude of about 64 degrees. These locations are about 4 cm below the Fp1/2 level and about 3 cm from the midline -- almost exactly over the corneas of the eyes. There were slight differences in these positions between the different recordings and very significant differences in the orientations of the dipoles.

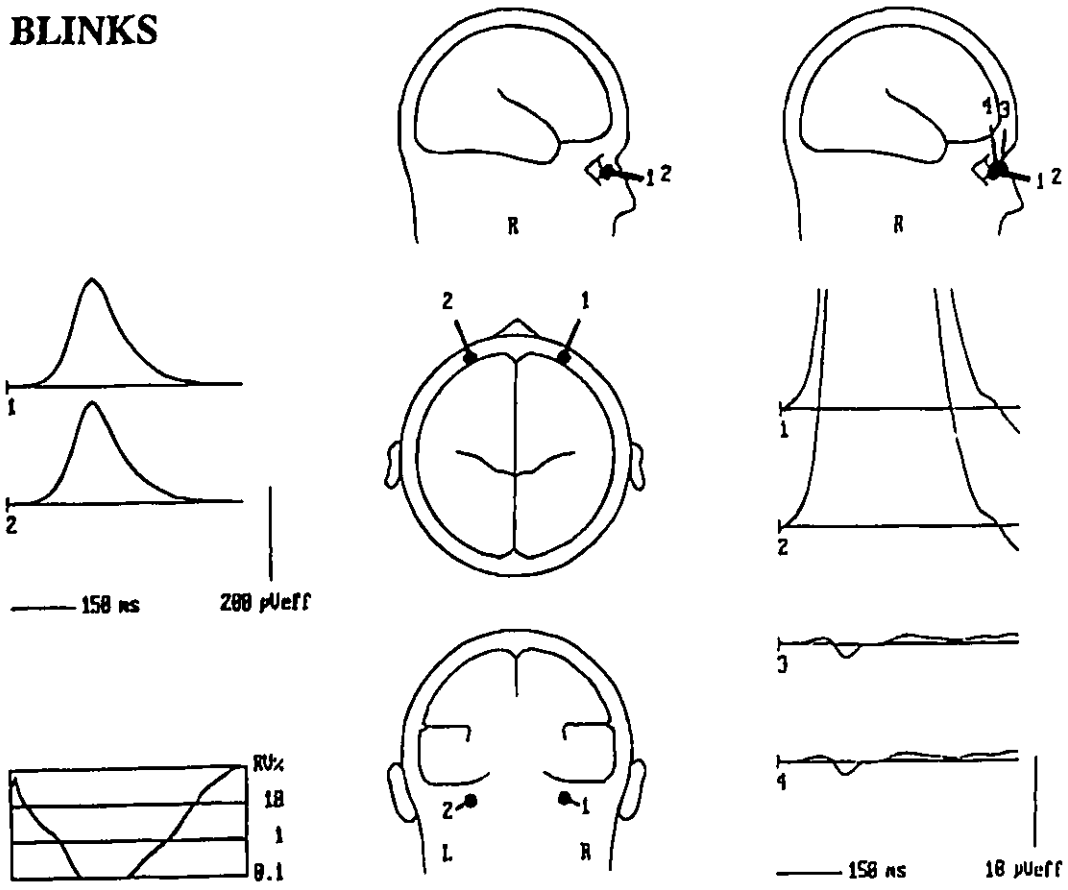

Figure 12: Blink dipole solution. This figure shows that blinks can be well modeled by two dipoles, one at each eye. The left column shows the source potentials. The residual variance (RV%), shown below the source potentials, is the amount of variance in the data not explained by the model. Two-dipole models for the blink potential are very stable and the residual variances are below 0.3%. As seen in the middle column of the figure, the dipoles are located close to the corneas of the eyes and point forward. In order to see if there were any concomitant vertical eye-movements with the blinks we added the up-2 dipoles, with the result shown at the right side of the figure on a much larger vertical scale. The up-2 dipole does not "attract" much activity or significantly affect the residual variance. The waveforms suggests a small downward deflection (about 1,6°) of the eyes at the beginning of a blink.

The two-dipole blink solution (blink-2) showed dipoles that were oriented horizontally and slightly downward (theta = 100°±1°). The two-dipole solution for the up-saccade (up-2) showed dipoles that were oriented vertically and a little posteriorly (theta =-14°±13°). This can be seen in Figure 12 (center) and Figure 13 (left).

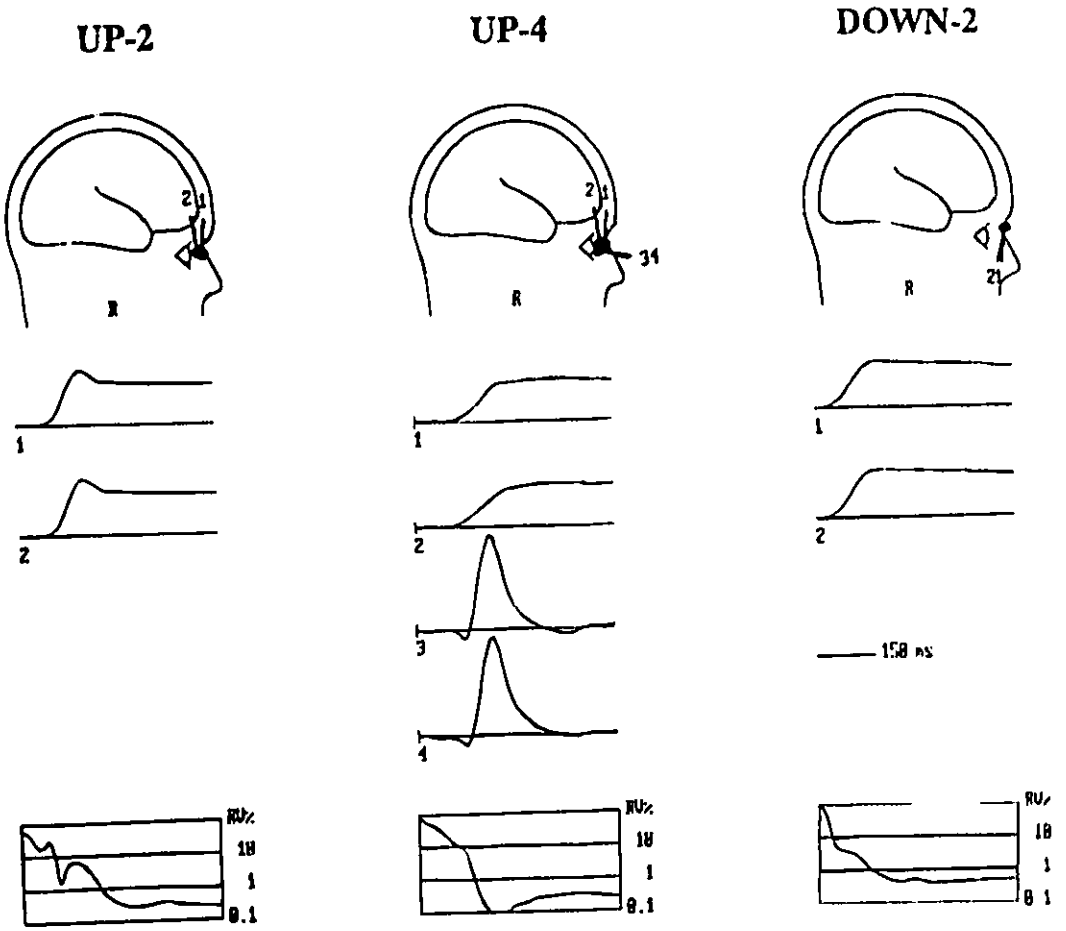

Figure 13: Vertical saccade dipole solutions. The left column shows the 2-dipole solution for the vertical saccades. The residual variance is high at the initial part of the saccade, during the rider artifact. To test the hypothesis that rider artifact at the beginning of the up-saccade is generated by a mechanism similar to the blink, we added the blink dipoles to the up-2 solution and then fitted to the initial portion of the saccade. This provided the up-4 solution shown in the middle column. The residual variance in region of the rider artifact is now reduced to near zero. The right column shows the 2-dipole solution for the down-saccade.

We attempted to explain the rider artifacts in the up-saccades by adding two more dipoles to the 2-dipole solution to give a new solution ("up-4") that explained significantly more variance. The additional dipoles in this solution turned out to be very similar to the dipoles of the blink solution (Figure 13, center). Conversely, adding the 2 up or down dipoles of the vertical saccades to the blinks dipoles showed a small initial downward deflection of the eyes during a blink (Figure 12, right). The amplitude of this movement was approximately 1.6°.

Figure 14 shows both the up and down saccades viewed through a model that combined the up-2, down-2 and blink solutions.

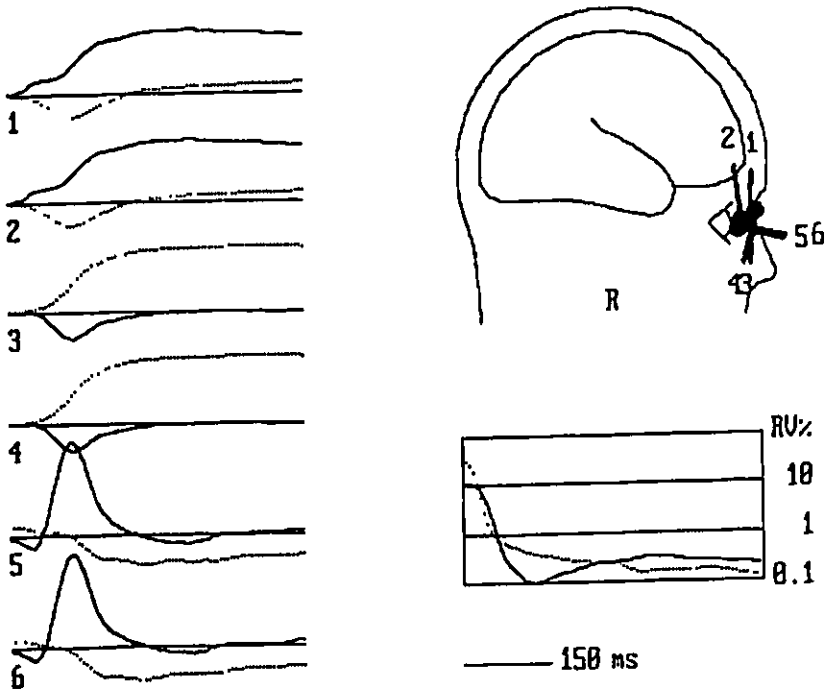

Figure 14: Vertical saccades. This figure shows the up and down saccades (20°) as viewed through a combination of the up-2, down-2 and blink solutions. The up-saccade potentials are plotted as continuous lines and the down-saccades are plotted as dotted lines. Note that the blink dipoles (dipoles 5 and 6) are very active during the rider-artifact and greatly decrease the residual variance of the up-saccade model during this segment. During down-saccades, the blink dipoles are active a little through the duration of the saccade. Also note that the down-saccades dipoles are active at the onset of the up-saccades and that the up-saccade dipoles are active slightly at the onset of the down saccade.

The two-dipole solutions for the horizontal saccades showed dipoles that pointed laterally and backward for the abducting eye and medially and slightly forward (toward the nose) for the adducting eye. Adding two more dipoles improved the fit. These extra dipoles were essentially the same as the blink dipoles and showed waveforms similar to the rider artifacts of the up-saccades, although smaller. As seen in Figure 15, the amplitudes of these source potentials were significantly greater for the abducting eye.

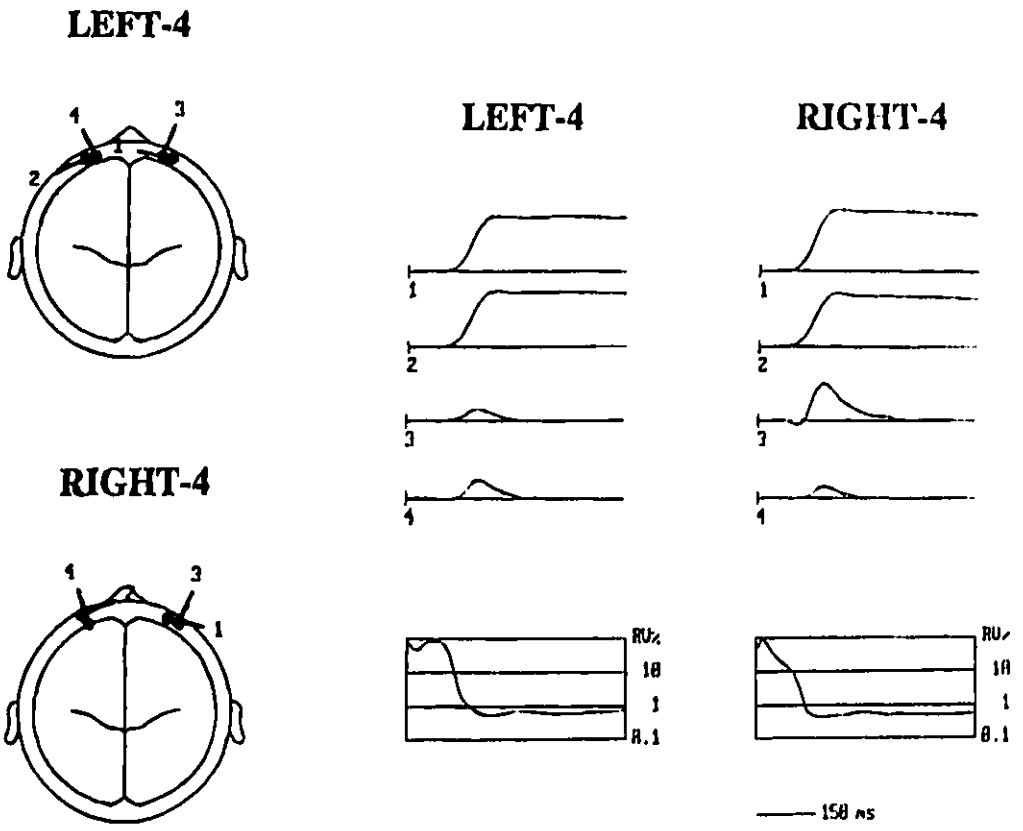

Figure 15: Horizontal saccade dipole solutions. This figure shows the 4-dipole solutions for the 20° horizontal saccades. An asymmetrical eyelid effect (dipoles 3 and 4) occurs at the beginning of the saccades. The source potentials of the blink dipoles are larger at the side towards which the eye moves. This probably occurs because the eyelid is more elevated at the middle than at the sides and the medial part of the lid is more elevated than the temporal part. As the eye moves horizontally, the cornea starts to go under the lid until the lid is elevated a little. These models were obtained by adding the blink dipoles to the right saccade and left-saccade 2-dipole models and fitting the blink dipoles over the initial part of the saccade.

Source components

Figure 16 shows the source components derived from principal component analysis of the recordings obtained during blinks and saccades using two different techniques -- PCA-1 and PCA-3.

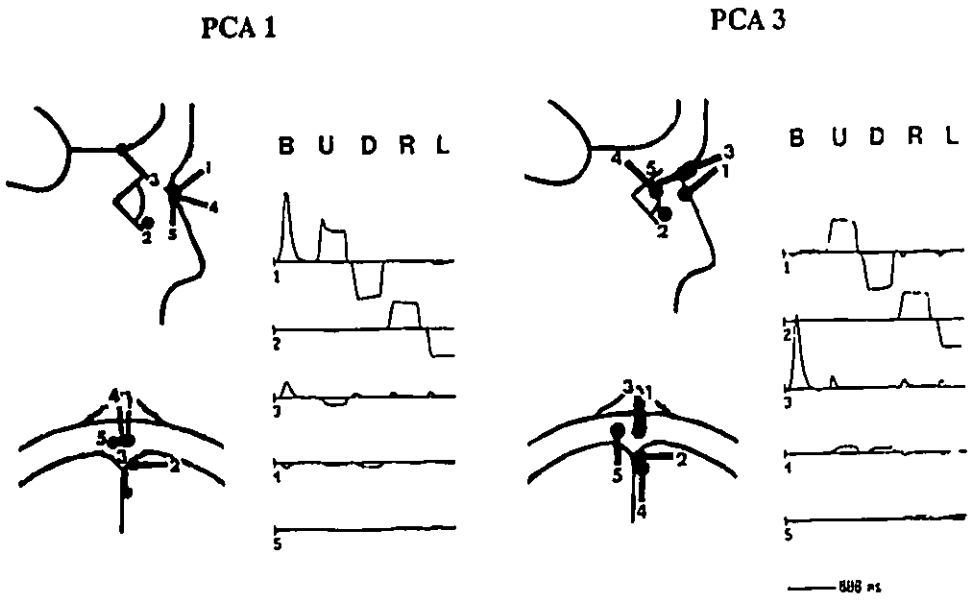

Figure 16: Source components. The source components were derived from a PCA of the ocular calibration waveforms. These waveforms spliced together the average waveforms for blinks, up-saccades, down-saccades, right-saccades and left-saccades. In the PCA-1 method the PCA was performed over the entire data. Note that the components do not correspond one-to-one to a single type of ocular activity. In the PCA-3 method three separate PCAs, for blinks, vertical saccades and horizontal saccades, were performed. The first component for blinks, the first two components for the vertical saccades and the first two components for the horizontal saccades were than combined. As can be seen the first and second components of the PCA-3 solution models most of the variance in the vertical and horizontal saccades while the third component model the blinks. The fourth and fifth components contribute to the saccades. The fourth component represents the fact that the equivalent dipoles for the up and down saccades point a little backward as well as vertically. The fifth component does the same for the horizontal saccades. These components have been specifically selected to represent the different types of eye movements. One can thus evaluate simultaneous activities in different source components. During a blink, there is a small downward deflection in the first component representing vertical eye movements. During upward and left and right saccades there are small deflections on the blink component representing the rider artifacts.

In PCA-1 a single PCA was performed on the whole waveform combining blinks, vertical saccades and horizontal saccades, whereas in PCA-3 separate PCAs for blinks, vertical saccades and horizontal saccades were performed.

In PCA-1 the first five components from the PCA of these data were chosen. This was based on the fact that these components had morphologies related to the eye movements. Later components were often located at some distance from the eyes. They probably explained residual brain and muscle activity in the recordings. The five factors explained 96±1% of the variance, with the individual factors accounting for 43±3, 37±2, 9±2, 5±1 and 2±1% of the variance. These factors could be plotted on the head model as if they were dipoles (Figure 16 -- PCA-1).

Two basic patterns resulted, each occurring in four of the eight subjects. In both patterns, the third factor was oriented radially and picked up variance from the blinks (and some of the eye movements). In the first pattern the first and second factors were oriented vertically and horizontally (in 3 subjects the first factor was vertical and the second factor horizontal, and in the fourth subject the first factor was horizontal). In the second pattern the factors were oriented diagonally relative to the vertical and horizontal axes. (A varimax rotation of these factors would make them almost identical to those of the first pattern.) The blink variance was shared between the third factor and the vertical-saccade factor. The analysis of the grand-mean data shown in Figure 16 showed the first pattern of results.

In PCA-3, separate factors for the blinks, the combined vertical saccades, and the combined horizontal saccades were derived. In these analyses, the first factor for the blink

that accounted for 84±13% of the recorded variance, the first two factors for the vertical eye-movements (77±5 and 13±4%) and the first two factors for the horizontal eye-movements (81±5 and 10±4%) were chosen. We then combined these five factors to give a PCA-3 set of ocular source components.

This final set of factors was similar to the first pattern of factors obtained from the combined data sets. The major difference was that the blink factor was more clearly separated from the vertical saccade factor. The factors in this solution were not orthogonal and could therefore separately portray the different kinds of ocular artifact. The vertical and horizontal eye movements were each represented on two components: one picking up the tangential variance and its direction, and the other picking up the radial variance (a saccade involves rotation oriented both in the direction of the saccade and toward the center of the rotation).

As can be seen in Figure 16 -- PCA-3 it was possible to read from the component waveforms what eye or lid movements had occurred. The first component, representing vertical eye movements, shows the small downward eye movement that occurs at the beginning of a blink. The third component, representing lid movements, shows the rider artifacts that occur at the beginning of saccades in the up, left and right directions but not down direction.

DISCUSSION

Dipoles in a Volume Conductor

Some theoretical aspects of dipoles will be helpful for the following discussion. As shown in Figure 17, the rotation of a dipole in a volume conductor is equivalent to the addition of a dipole with a magnitude and direction equal to the vector subtraction of the dipole in its final position from the dipole in its initial position. The larger the rotation, the larger the equivalent dipole and the more it points "backward" from the initial dipole. Thus, the magnitude of the rotation will affect both the size and the orientation of the equivalent dipole. The effects of changing the initial location of the dipole are shown on the right half of the figure. What is recorded at a particular location in the volume conductor depends on the location of the recording electrodes relative to the dipole and on the initial orientation of the dipole.

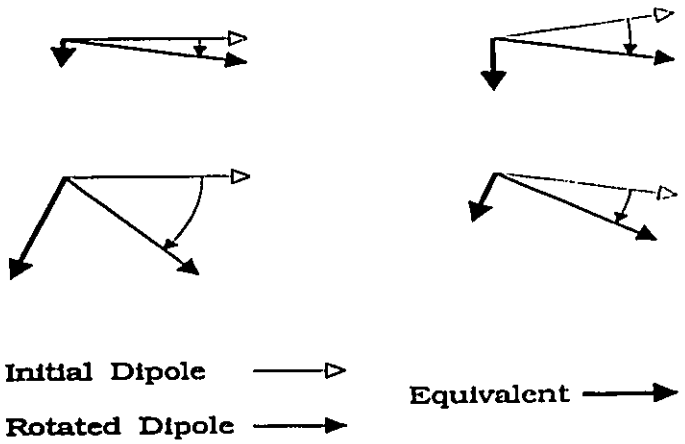

Figure 17: Rotating dipoles. The diagrams in this figure illustrate the changes that occur when a dipole rotates in a volume conductor. The upper left diagram shows that the rotation of a dipole from one orientation to another is equivalent to the addition of a dipole oriented along the vector difference of the initial and final orientations. The lower left diagram shows a larger rotation. As well as being larger, the equivalent dipole is pointed more backward from the initial dipole than the smaller rotation. The right diagrams show how the initial position of a dipole affects the equivalent dipole for rotation.

The BESA programs use a three-shell head model. Although this is quite accurate for localizing source dipoles within the brain, it is not accurate when localizing the ocular dipoles since these are located outside the skull. The main inaccuracy occurs in calculating the eccentricity of the dipoles which is overestimated. The locations are otherwise fairly accurate -- the actual dipoles are just located further away from the surface than the calculated dipoles. The orientations of the dipoles are quite accurate.

Source dipoles and source components for blinks and saccades

Source dipoles for blinks and up-saccades are different - blink dipoles are oriented forwards whereas up-saccade dipoles points upwards. Blink and vertical saccade source components are also different , especially after a varimax rotation. This clearly indicates that different mechanisms generate blink and saccades. As discussed previously, an upward rotation of a dipole in a volume conductor generates an equivalent dipole that is oriented upwards and more or less backwards, depending on the magnitude of the rotation. That corresponds with the dipoles obtained for up-saccades (Figure 13, left). Blink dipoles have a clearly different orientation -- they point forward (Figure 12, center). This orientation is what would be expected to be generated by the "sliding electrode" mechanism. As the eye lid slides down the positively charged cornea the flux of current through the lid increases. The net current flow during the movement of the lid would be oriented approximately forward.

Vertical eye movements during blinks

If we combine vertical movement dipoles to blink dipoles we can test for the occurrence of vertical eye movements during a blink (Figure 12, right). we can even

estimate the amount of movement by measuring the source potential amplitude for the 20° saccades and calculating a conversion factor from microvolts in the source potentials to degrees of eye movement. We found that the eyes apparently moved downwards by about 1.6° during a blink. The source component representing vertical eye movement also shows a small downward eye movement at the beginning of a blink (Figure 16, PCA-3, component 1). This finding of a small downward movement rather than an upward movement is similar to those obtained using other techniques (Evinger et al., 1984; Collewijn et al. 1985). One possible explanation might be friction between the lid and the eye.

Rider artifacts

Barry and Jones (1965) showed that the distortion that occurs at the onset of vertical saccades (the "rider artifact") is most probably caused by the eyelid. The eye moves upwards a little before (Becker and Fuchs 1988) or a little more rapidly (Barry and Jones 1965) than the eyelids during an up-saccade. Thus, at the beginning of the movement the eye slides a little under the eyelid. This "reverse blink" mechanism increases the positivity at the forehead.

If the rider artifact corresponded to a saccade overshoot followed by a correction saccade, the dipoles of this part of the up-saccade would be similar to vertical saccades. However, the rider artifact is not well modeled by up-saccade dipoles (Figure 13, left). Note the higher residual variance during the rider artifact. Down saccade dipoles also do not model well the rider artifacts (Figure 14, dipoles 3 and 4). Furthermore, the source

component representing vertical eye movements does not show the rider artifact (Figure 16, PCA-3, component 1). Therefore, it is not likely that the rider artifact is generated by the same mechanism as vertical saccades, as would be expected in the case that the rider artifact was generated by a saccade overshoot.

We tested Barry and Jones hypothesis that the "rider artifact" is generated by the eyelid by adding blink dipoles to the Up-2 solution. These blink dipoles modelled the rider artifacts very well (Figure 13, center, dipoles 3 and 4). Notice that the residual variance is reduced to near zero in the period of the rider artifact. As well, the source component representing lid movements also clearly shows the rider artifact (Figure 16, PCA-3, component 3). The rider artifact is not noted during down-saccades (Figure 13, right and Figure 16, PCA-3). The Matsuo et al. sliding electrode hypothesis, thus, explains both the generation of blink potentials and the rider artifact during up-saccades.

We also found a similar process during horizontal saccades. When the eyes move to the left or to the right, they move away from the widest part of the palpebral fissure. A small upward movement of the lid would therefore be necessary to maintain unimpeded gaze. Because of the shape of the palpebral fissure this eyelid movement might be larger for the abducting eye. As with the up-saccades, the lid movements might lag slightly behind the lateral eye movements to cause a small rider artifact. Shortly after the new eye position is reached, the lid moves upward, resulting in a return of the rider artifact to baseline. The rider artifacts associated with the lateral eye movements show up clearly in Figure 15 (dipoles 3 and 4) and Figure 16 (PCA-3, component 3). The eyelid movements associated with lateral saccades are small and have not been noted before.

Asymmetries in saccade potentials

We found a consistent asymmetry between the ocular potentials for right- and left-saccades (Chapter 2). Measurements from the third experiment showed that right saccades had significantly larger amplitudes at the external canthus of the right eye and left saccades at the external canthus of the left eye. Recently, Häkkinen et al. (1993) also observed a significantly larger amplitude in horizontal and oblique eye movement potentials recorded at EOG electrodes toward which the eyes moved as compared to the opposite electrode.

These findings are probably related to the manner in which electrical fields change when a dipole rotates in a volume conductor. When the rotation occurs, the field changes its orientation (but not its location). As can be seen in Figure 17, the effect is equivalent to the creation of a new dipole with the same location and with an orientation and size that are the vector difference between the initial and final orientation. As the figure illustrates, a small movement causes an equivalent dipole that is almost perpendicular to the initial dipole, whereas a larger movement causes an equivalent dipole that points a little backwards from the initial dipole.

Unfortunately, we do not know the orientation the equivalent dipole of the eye when the eyes are gazing straight ahead. It is possible that the coverings of the eye and the optic nerve may cause this resting dipole to be oriented a little laterally. The eyeballs are surrounded by fat, bone and air, which are effective electrical insulators. The fluxes of ocular currents out of the orbit occur largely through its open anterior pole and through the posterior optic nerve. If the resting dipoles were indeed oriented a little laterally to straight ahead, the equivalent dipoles for the rotation of the abducting and adducting eyes

would be differently oriented -- the abducting eye would be pointing laterally and backward whereas the dipole for the adducting eye would be pointing medially and perhaps a little anteriorly. The potentials recorded at homologous sites lateral to the eyes would be different -- with a larger potential near the abducting eye. These predictions fit the dipole sources derived for the lateral eye movements (Figure 15, dipoles 1 and 2).

Up-saccades had similar amplitudes above and below the eye, whereas down-saccades resulted in larger amplitudes above the eye. If the resting dipole of the eye points a little down from straight ahead, the equivalent dipole for a downward movement would be oriented more posteriorly than for an upward movement. This would fit with the dipoles obtained (Figure 14, dipoles 1, 2, 3 and 4) and would explain the asymmetries of the potentials near the eyes during vertical eye movements.

4

CORRECTION METHODS

INTRODUCTION

Ocular artifacts are a potentially serious problem when recording EEGs and event-related potentials. For EEGs they can obscure frontal recordings and mimic pathology in the anterior regions of the brain. They are a particular problem for the computer analysis of the EEG since present programs cannot easily distinguish EOG from EEG (Lee and Buchsbaum 1987; Hughes and Miller 1988). For the event-related potentials, ocular artifacts may significantly distort the averaged waveform, since these artifacts can be large and are easily entrained by stimuli (Hillyard and Galambos 1970; Picton 1987).

The most widely used methods to remove ocular artifacts subtract part of the EOG signal from the EEG or ERP signal (Jervis et al. 1988; Ifeachor et al. 1988). The fraction of the EOG that contaminates each EEG electrode is obtained by calculating propagation factors as the slope of the best fit straight line relating the EOG with the EEG signal at any particular EEG electrode location and using them to scale the EOG signal before it is subtracted from the EEG (Hillyard and Galambos 1970). Unfortunately, the EOG electrodes pick up some activity from the brain, as well as activity from the eyes. This EEG activity will be partially subtracted out (as well as the EOG) from the scalp recordings (Berg and Scherg 1991b; Berg et al. 1992).

Dipole source analysis might help to overcome this problem since it can postulate separate sources for both the EEG and the EOG. The EOG activity is modeled using source dipoles located at the eyes (Berg and Scherg 1991a). These dipoles can model the potentials generated in the eyes and thereby remove them from the recorded EEG. However, EOG compensation by dipole analysis has some difficulties. Present programs for source analysis use a simplified three-shell model of the head. The inaccuracies of this model near the eyes can lead to inaccuracies in the location of the sources and in the assessment of their contribution to the scalp-recorded fields.

Principal Component Analysis (PCA) calculates components underlying scalp recorded waveforms without the constraints of head models. Although not giving information about the location and orientation of intracranial generators, PCA may work better for the purpose of removing ocular artifacts, because it may provide a better description of the ocular artifacts present at each electrode site. Berg and Scherg (1991b, Berg et al. 1992) have recently proposed a technique for removing ocular artifacts using PCA. In this technique the EOG potentials are modeled by source components obtained by PCA. The EOG source components are similar to the forwardly modeled eye dipoles (or a linear combination of these). Because they are experimentally calibrated for each subject, they can compensate precisely for the distortions of the volume-conductor model near the eyes.

In this chapter, we compare different techniques of correcting for EOG artifacts, based on EOG propagation factors, source dipoles and source components.

METHODS

Recordings

These studies use data from the third experiment described in Chapters 2 and 3.

Test files

In order to evaluate the effectiveness of the different techniques for compensation we made up a test file for each of the eight subjects in the third experiment. This test file averaged together five different recordings. Four contained saccadic eye movements in each of the four directions. The timing of the saccade was altered so that the saccades did not exactly overlap, but occurred in the order: up, right, down, left. The fifth recording contained between 4 and 8 blinks randomly located through the recording sweep. Two different versions of this file were created, one with all of the referential EOG channels and one with differential VEOG and HEOG channels as in the second experiment. The VEOG channel was obtained by subtracting the recordings from the left lower eye from the recording from the left upper eye, and the HEOG channel was formed by subtracting the right canthal recording from the left canthal recording.

Correction Procedures

Five different EOG compensation techniques were evaluated on these test files: The first technique (*"regression-1"*) applied one set of vertical and horizontal EOG compensation factors to the data without distinguishing between blinks and vertical saccades. We arbitrarily chose to use the vertical saccade compensation factors rather

than the blink compensation factors for this procedure. The second technique (*"regression-2"*) involved two steps. The recording wherein the blinks occurred was compensated using the blink compensation factors and then averaged with the four different saccade recordings. The combined data were then compensated using the vertical and horizontal EOG compensation factors for saccades. The third technique ("*dipole*") modeled the effects of ocular dipoles on the recordings using BESA. Six dipoles were used to model the ocular potentials. The process only works properly if the EEG sources in the brain are simultaneously modeled. The ocular and cerebral sources then "compete" for the recorded variance. Because six dipoles were already been used to model the EOG potentials, only two regional sources (Scherg and Picton 1991) -- three dipoles with the same location and orthogonal directions -- could be used to model the EEG. One was located in each hemisphere on the coronal plane (phi=0°), with an eccentricity of 55% and an azimuth of ±80°. The fourth and fifth techniques ("*PCA-1*" and "*PCA-3*") used the EOG weighting functions calculated with the source components technique of Berg and Scherg (1991b) discussed in Chapter 3, using 2 different sets of source components, as will be described in a moment.

The regression corrections used propagation factors calculated as described in Chapter 2. To obtain vertical and horizontal differential EOGs from the referential recordings in experiment 3, we subtracted the upper left EOG channel from the lower left EOG channel and the left canthus EOG channel from the right canthus EOG channel, respectively. Propagation factors were calculated for each individual subject. The propagation factors were used to scale the EOG signals to obtain the fraction of the EOG present at each EEG electrode. These fractions were then subtracted from the recorded EEG to obtain the corrected EEG.

For the purpose of correction of EOG artifacts with source dipoles we modelled the data set that combined blinks and saccades in 4 different directions using six independent dipoles. This model ("all-6") used 3 pairs of dipoles (3 dipoles for each eye) to fit the vertical eye movements, the horizontal eye movements and the blinks over their respective epochs. First, the two dipoles from the blink solution were combined with the 2 dipoles from the up-2 solution (see part 1 of this paper). Then, the dipoles of abducting eye from each of the left-2 and right-2 solutions were added. Finally, each of the three pairs of dipoles was fitted during their respective epoch (blink, vertical saccades and horizontal saccades). Only the dipole pair that was maximally active during each of the three epochs was switched on during the fitting.

For the corrections using source components a PCA was performed on the combined data sets. This provided a set of source components. The weighting factors of each of these source components at the different electrodes could then be used in conjunction with the dipoles used in the forward solution of the EEG sources. Two different techniques were used to assess the source components and weighting functions, PCA-1 and PCA-3: The first approach (PCA-1) was to perform a principal component analysis of the combined data set from all of the different eye movements. The first five components of this analysis were chosen to provide us with a set of EOG source components (in preliminary studies just the first three components were also tested). In the second approach (PCA-3), the blinks, the vertical eye movements and the horizontal movements were separately analyzed, i.e., three different PCAs were performed. Then, the first component (explaining most of the recorded variance) for the blink and the first two components of each of the vertical and horizontal eye movements were selected and combined into one set of five VEOG coefficients.

The weighting functions for the ocular source components could be compared to the propagation factors calculated by linear regression of the vertical and horizontal EOGs on the scalp-recorded data. The propagation factor at a particular electrode location equals the weighting coefficient at that location divided by the difference between the weighting coefficients for the two electrodes contributing to the bipolar EOG recording.

Plotting conventions

The scalp-recorded data are plotted negative up. The waveforms showing the activity of the dipole source or the source-components in time are plotted positive up.

Data analysis

The data was evaluated by assessing the root-mean-square amplitude of the corrected recordings at each of the scalp locations. This measurement assessed the amount of EEG and residual EOG present in the recordings. It would be reduced as the EOG was compensated (and increased if the EOG was overcompensated or undercompensated). Repeated measures ANOVA with Greenhouse-Geisser adjusted degrees of freedom and Tukey honestly significant difference (HSD) test were used to compare the results of the EOG compensation. A significance level of $p<0.05$ was used.

RESULTS

The propagation factors used in the regression-1 and regression-2 methods are tabulated in column 2 of Tables 4 and 5 (Chapter 2).

The dipoles of the six-dipole solution ("all-6") used in the dipole method are described in Table IX and illustrated in Figure 18. The figure actually shows the fit of the grand-mean waveforms across all the subjects and is slightly different from the dipole data in the table. The figure also shows the source waveforms and the residual variance. One pair of dipoles weights heavily on the blinks and also picks up the rider-artifacts on the up-saccades and the horizontal saccades. The other dipoles model the vertical and horizontal saccades. Attempts to model the ocular potentials using more than 6 dipoles were unstable since similarly oriented dipoles tended to interact.

Figure 16 (Chapter 2) illustrates source components as the ones used in the PCA-1 and PCA-3 corrections methods. This figure shows the analysis of the grand mean data.

Table IX: Source dipoles for the six-dipole model. Only the right-eye dipoles are shown. The left-eye dipoles were symmetrical in both position and orientation to the right-eye dipoles. *Eccentricity* is expressed as a percentage of the radius of the head model. *Theta* and *Phi* angles for the *locations* and *orientations* are in degrees. *Residual Variance* is the percentage of the recorded variance unexplained by the dipole model.

EOG	Sources					RV
	Location			Orientation		
	Ecc	Theta	Phi	Theta	Phi	
All-6	100±0	114±2	62±2	101±3	64±4	
	96±4	112±5	72±5	-17±14	17±26	
	99±2	110±4	63±2	93±14	-17±14	0.5±0.2

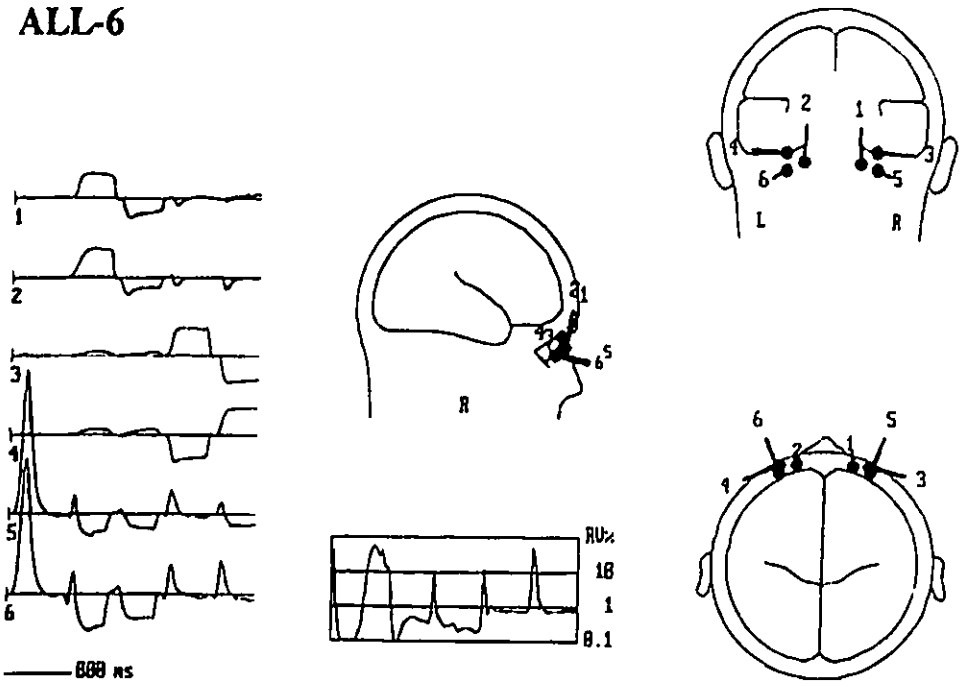

Figure 18: Six-dipole solution for all eye movements. On the left are shown the dipole sources modelling the grand-mean waveforms that combined together the blink, up and down saccades and left and right saccades. The first two sources model most of the variance in the up and down saccades. The second pair of dipoles picks up most of the variance in the horizontal saccades. The fifth and sixth dipoles model the blinks and the rider artifacts at the beginning of the up-saccades and the horizontal saccades. These radially oriented dipoles also pick up some of the variance in all of the saccades. Since the dipoles for up and down saccades are differently oriented, using one pair of dipoles to model both leaves some residual variance unaccounted for and this is picked up by the blink dipoles.

Methods of comparing the corrections methods

One way to compare the different correction procedures was to see how well they corrected the grand mean data for all the different eye movements used in calculating the different correction factors. This is shown in Figure 19. As can be seen, the two different PCA procedures gave much better corrected waveforms than the other techniques.

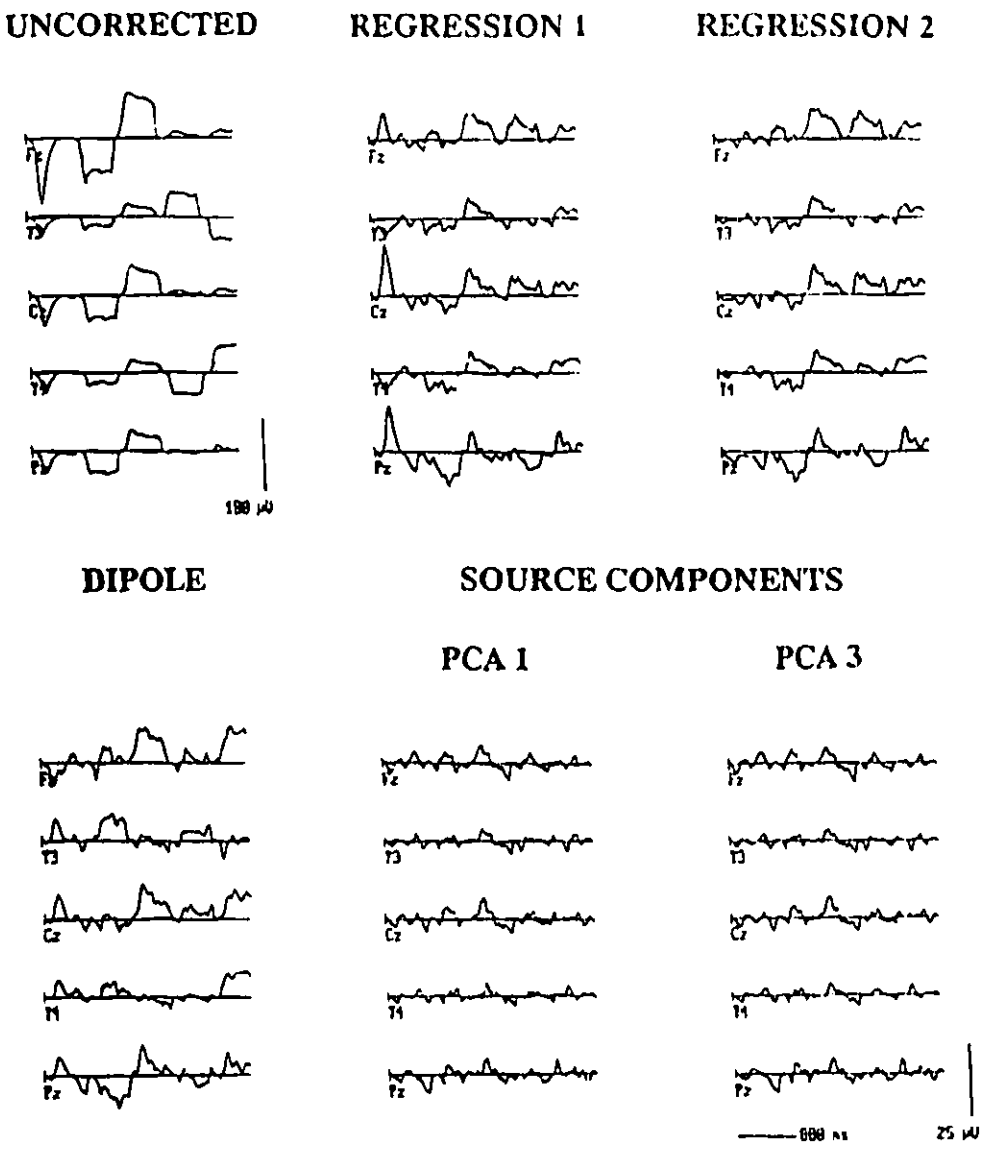

Figure 19: Correction techniques. This figure compares the five correction techniques on the grand-mean waveforms actually used to calculate the dipoles and source components illustrated in the previous two figures. Uncorrected data are shown in the upper left of the figure. The corrected waveforms obtained with different techniques are shown in the rest of the figure. Different scales are used for plotting the uncorrected and corrected data. Notice that the Regression 1 method (correction using only the saccade vertical propagation factor) introduces opposite polarity blink artifacts at the more posterior electrode sites because saccades factors for those sites are larger than blink factors. The Regression 2 method (which corrects blinks before correcting for saccades) compensates blinks much better. Note that the rider artifacts at the up-saccades and horizontal saccades are not well compensated. The 6-dipole method did not work so well because two vertical dipoles cannot adequately model both up and down saccades and two horizontal dipoles cannot adequately model both left and right saccades. Furthermore, the simple three-shell head model is not correct when modelling the ocular dipoles accurately. The source components techniques that derive from a PCA of the ocular waveforms method appear to work best.

The different correction procedures were also evaluated by assessing the root-mean-square (RMS) amplitude of the corrected "test" waveforms. An example of the test waveforms for one subject is shown in Figure 20.

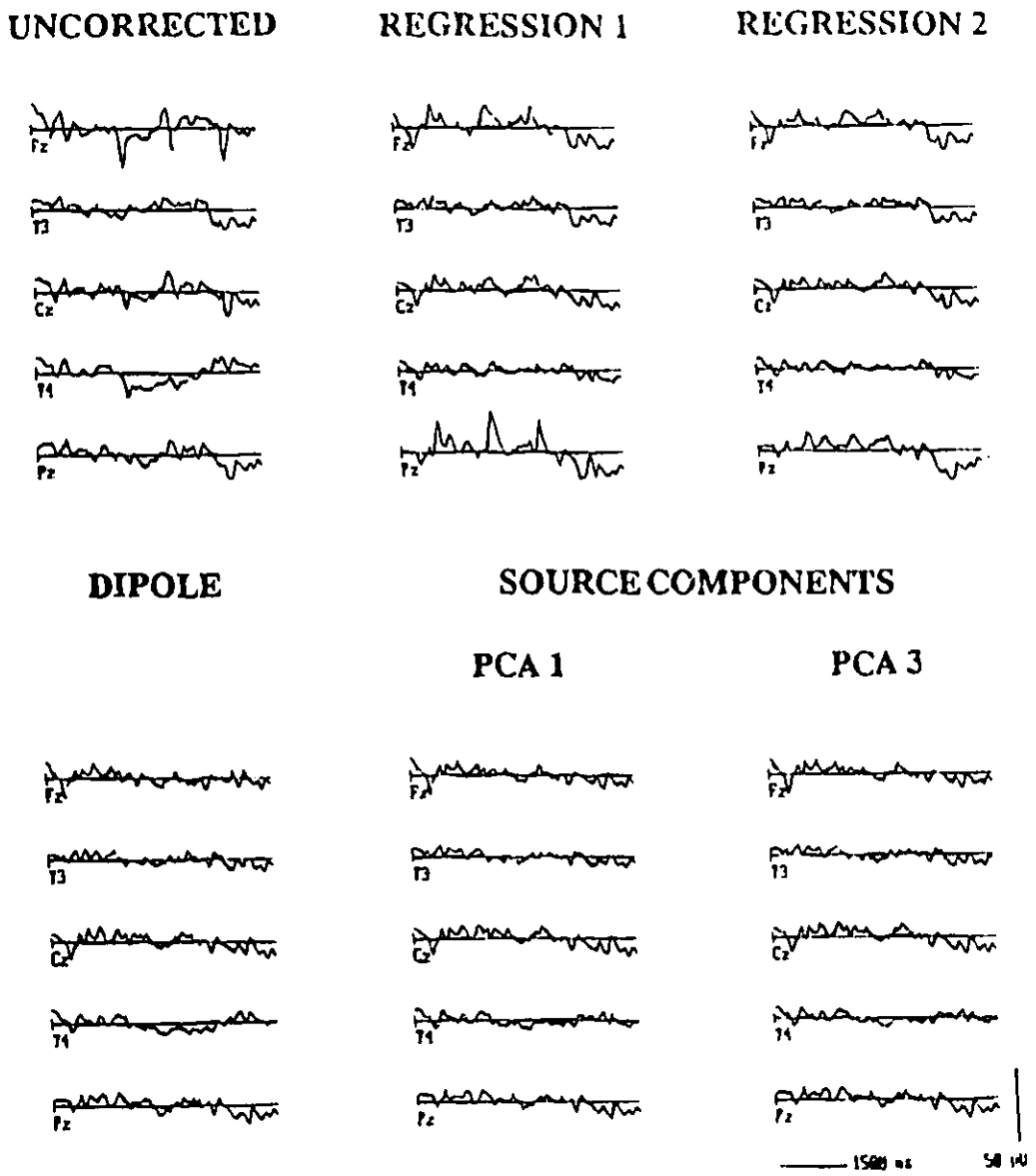

Figure 20: Correction techniques on the data from an individual subject. This figure is set up in the same way as the preceding figure. However, these data were not the same data as were used to calculate the regression factors or source components. Rather they were "test" recordings obtained by averaging together single trials without any time-locking. Furthermore, these data are not the grand-mean data from all subjects but rather the data from a single typical subject.

The mean and standard deviations of the RMS amplitudes at the scalp electrodes for the 5 correction methods are shown on Table X.

Table X: Root-mean-square amplitude (μV) of the corrected "test" waveforms.

Location	Regression-1	Regression-2	Dipole	PCA-1	PCA-3
Fz	8.6±1.2	7.6±0.8	6.6±0.7	5.3±0.4	5.6±0.6
A1	7.1±1.8	6.3±1.4	4.8±0.7	4.2±0.7	3.9±0.7
T3	7.5±1.3	6.6±0.9	4.8±0.5	5.0±0.6	5.0±0.7
C3	8.2±1.2	7.5±1.0	6.3±0.8	6.1±0.5	6.2±0.8
Cz	7.9±0.8	7.0±0.7	6.2±0.6	6.3±0.6	6.0±0.5
C4	7.6±1.1	7.4±1.0	6.4±0.7	5.9±0.5	5.6±0.6
T4	7.3±1.6	7.1±1.8	6.0±1.2	5.5±1.0	5.5±1.2
A2	6.3±1.9	5.8±1.5	4.0±0.7	3.3±0.4	3.3±0.5
Pz	10.3±2.0	9.1±1.8	6.9±0.9	6.2±0.6	6.4±1.0
Mean	7.9±0.5	7.1±0.4	5.8±0.3	5.3±0.2	5.3±0.3

The ANOVA showed a significant main effect for correction methods. Although the regression-1 technique had very high amplitudes at the Pz electrode there was no significant interaction between correction methods and electrode positions. The Tukey HSD post-hoc comparisons showed the following results:

1) The regression-1 procedure showed significantly higher residual amplitudes than all other techniques. As can be seen in figure 21 this technique tended to overcompensate for the blinks at posterior electrodes.

2) The regression-2 procedure (which separately compensated for blinks and saccades) was significantly better than the regression-1 technique but significantly worse than the techniques using dipoles or source components. If the source-component corrections were performed using three components rather then five, the difference between the regression-2 technique (7.1 μV) and the source component techniques (6.1μ V) were no longer significant.

3) Although the PCA techniques had lower RMS amplitudes then the dipole technique these differences did not reach significance.

4) The two different types of source-component correction -- using the three components from the combined data (PCA-1) or combining the separately analyzed blink and saccade factors (PCA-3) -- gave essentially identical results.

DISCUSSION

Three techniques for correcting the EOG artifacts when recording the EEG were evaluated: propagation factors, source dipoles, and source components. All can work reasonably well, although the source component approach was the most efficient and the most powerful.

A system to compensate ocular artifacts using *propagation factors* should distinguish blinks from up-saccades since these have different propagation factors. One procedure would be to distinguish blinks on single-trial recordings (or on-line), compensate these periods of the recording prior to averaging with blink propagation factors, and then compensate for the saccades on the average recording. Since blink potentials are generally larger than most up-saccade potentials, an amplitude criterion might work. For example, in the present data 95% of the blinks had amplitudes in the vertical EOG more than 160 μV. This is approximately the amplitude of a 13 degree up-saccade. A criterion of 160 μV would then correctly detect 95% of the blinks but incorrectly detect saccades greater than 13 degrees. These amplitude criteria would have different values if one uses referential derivations using electrodes above or below the eyes instead of the vertical EOG. The major problems of an amplitude criterion are "incomplete" blinks (blinks with much smaller amplitudes than usual) and large up-saccades. Another approach would evaluate the rate of change of the slope (from positive to negative). Blinks can be detected by locating the time points in the EOG where the rate of change of the slopes calculated over 10 msec periods before and after the time-point exceeds a criterion (Gratton et al. 1983). The present results indicate that the differentiation would be better if longer time periods were used. However, we might then be confounded by a rapid return-saccade. In our experience the fastest a subject can

complete a saccade and a return to the resting position was about 300 ms. A possible computer algorithm could run three points A-B-C, with A and B separated by 50 ms and B and C separated by 150 ms, through the Vertical EOG recordings. If the voltage (B-A)+(B-C) exceeds 300 μV, a blink would be detected. If we wished to detect rider artifacts as blinks (and compensate them as blinks rather than saccades) we could use a B-C interval of less than 50 ms.

Another approach would be to distinguish the blink potentials from the saccade potentials on the basis of their scalp distribution rather than on their temporal characteristics. One way to do this would be to calculate three different propagation factors based upon EOG potentials recorded with a vertical, horizontal and radial orientation (Elbert et al. 1985). This technique can distinguish blinks from saccades and compensate each appropriately. The three-factor approach is much more efficient than trying to distinguish blinks from saccades and then applying different two-factor compensations. However, it still causes some of the frontal EEG to be subtracted from the recordings together with the EOG potentials.

This is the major problem with using propagation factors: It is impossible not to subtract out some portion of the frontal EEG as well as the EOG. This is a separate problem from the EEG contamination of the EOG when calculating the propagation factors. As we have already discussed in preceding paragraphs, this contamination can be attenuated by averaging and filtering the EOG signals before calculating the propagation factors. The remaining problem is that the EOG signal being monitored during the experiment contains some EEG in addition to the EOG. Some portion of this EEG will then be subtracted out in the compensation process. There is no real way to prevent this. The problem can be attenuated by only applying the EOG correction process if there is an eye movement. In this way, the ongoing EEG that occurs continuously in the EOG

channels even when there are no eye movements will not be unnecessarily subtracted away. However, this only attenuates the problem and the amount of distortion will vary with the number of trials that are contaminated by ocular artifacts.

As the scalp distribution of vertical saccades and blinks are clearly different, any approach that attempts to compensate for both blinks and vertical eyes movements using only one set of propagation factors (e.g., Semlitsch et al., 1976), or only a single analog compensation process (e.g., McCallum and Walter, 1986), is doomed to failure unless the subject only blinks and does not move the eyes (or vice versa).

Source dipoles allow both the EEG and the EOG to be modelled simultaneously. This technique is better than propagation factors because it does not subtract out the frontal EEG signals with the EOG potentials (Berg and Scherg 1991b; Berg et al. 1992). Frontal EEG generators (or other generators causing potentials that are recorded over the frontal scalp) can be modeled simultaneously with the ocular potentials. The use of dipoles to model the EOG activity has some drawbacks. These are basically related to the fact that the three-shell head-model is not accurate for modelling ocular potentials. First, the geometry of the skull around the eyes is quite different from a sphere. Second, the ocular dipoles are located outside rather than within the skull. These problems lead to inaccuracies in the location of the dipoles and make it impossible to predict accurately the contribution of these dipoles to the different electrode locations.

Calculating *source components* can alleviate these problems. This approach does not seek to localize dipole sources. Rather it calculates the effects of eye movements at each of the scalp locations and expresses these effects in terms of a weighting function. These functions can represent the ocular contributions at each electrode location without the need for a dipole explanation. The weighting functions can be modelled with dipoles

at particular locations near the eyes, but this is only a best-fit procedure -- a "center of gravity" rather than a precise location and orientation. Evaluating EOG artifacts using source components has two major advantages over the dipole approach. First, it is more accurate since it does not have to force the EOG patterns into specific dipoles. Second, it can use fewer components to represent the EOG activity. Using three or five source components is just as effective as six-dipole sources in removing ocular artifacts.

Two techniques to calculate source components were evaluated. The two techniques were equally effective. The first technique performed a PCA on the data set that combined all the different types of EOG artifact. This has the advantage of being very simple. The second approach calculated different PCAs for blinks, for horizontal eye movements and for vertical eye movements. Although more complicated, this second technique does allow an easier monitoring of the types of eye movements been corrected in a particular recording since each source component is specifically associated with a specific type of eye movements.

The optimum number of source components needed for EOG correction is not known. The number of source components that should be chosen will vary with the number of peri-ocular recording electrodes, and the signal to noise ratio of the EOG signals (How many movements were combined? How large were the saccades?). Any component showing waveforms that are clearly related to the eye movements and having a location near the eyes should probably be chosen. If the waveforms are not related to the eye movements, the components are probably modelling EEG activity. If the components are not located near the eyes they may be modelling eye-related potentials generated in the brain rather then in the eyes.

For the present data, five components provided better correction than three components. This set of five source components includes a vertically oriented component for the vertical eye movements, a laterally oriented component for the horizontal eye movements and a radially oriented blink component. As well, there are two other radially oriented components. Single dipole sources for up and down saccades and for left and right saccades are not oriented in exactly opposite directions, but each points a little backwards. The fourth and fifth source components can represent this backward orientation of the saccadic dipoles.

Recommendations

These results indicate that the best approach to controlling for ocular potentials when recording the EEG or the event-related potentials is to calculate ocular source components. Although these components can be calculated from the eye movements during an experiment, it is recommended that this is best done in a separate ocular calibration recording. At this time, recordings are made using the same montage as will be used in the experiment. The head position and the direction of resting gaze should be the same as in the experiment. The optimum number of electrodes near the eyes is not known. The recording montage should probably include at least seven electrode near the eyes. Four of these electrodes could be at routine EEG locations: Fp1, Fp2, F7, F8. Electrodes on both cheeks below the eyes and an electrode at the nasion would make up the minimum complement.

During the ocular calibration the subject is asked to blink for a brief period and then to make saccades separately in the up, down, left and right directions. The size of the saccades should be between 15 and 20° to ensure that the ocular potentials contribute a greater part of the variance to the recordings than the EEG. If the up-down and left-right

saccades are combined, the size of the saccades should be approximately 30° (±15°). If possible, the multiple recordings from the blinks and from each of the saccades should be averaged together to give five average waveforms. The recordings should then be combined in some way to form an ocular data set. These average waveforms may be spliced together into one file, but it is also possible to use them separately.

Source components are calculated from the ocular data set. The optimum number of components is not known. We have found that five components is sufficient for excellent compensation and three components provide adequate compensation. One should probably choose those components showing waveforms related to the eye movements and located near the eyes. The source components can be separately calculated for each of the movements or types of movements (and combined later into a set of weighting functions), or calculated together from the combined data-set. Ultimately, the set of weighting functions is stored for use in analyzing or correcting the experimental data.

The source component coefficients can be used in two different ways. The first is to use them together with postulated dipole sources when performing a source analysis of the EEG or the event-related potentials. The weighting functions are then used together with the forward solutions of the postulated dipoles in modelling the recorded waveforms. This approach attempts to understand the activity of both the brain and the eyes during the recording. The second way of using the coefficients is to remove the ocular artifacts from a recording. When doing this one should place dipoles to model the EEG signals and then subtract out the signals that modelled on the ocular coefficients. Dipoles have to be placed for the EEG to prevent the problem that happens with propagation factors -- the subtraction out of EEG as well as EOG. If one has accurately modelled the EEG signals one can use these dipole sources. If not, one can use regional sources in regions of the

brain that generate the EEG. Once corrected, the EEG signals can be used for further analyses such as cross-correlation and spectral analysis.

Ocular artifacts have long been a problem in the recording of EEG signals. At times one spends more energy recognizing the artifacts from the eyes than interpreting the activity from the brain. The source component approach provides us with powerful and efficient techniques to evaluate and control these artifacts.

REFERENCES

Antervo A, Hari R, Katilla T, Ryhänen T and Seppänen M. Magnetic fields produced by eye blinking. Electroencephalogr. Clin. Neurophysiol 1985, 61: 247-253.

Arden GB and Barrada A. Analysis of the electro-oculograms of a series of normal subjects. Role of the lens in the development of the standing potential. Brit J Ophthal 1962, 46: 468-482.

Arden GB, Barrada A and Kelsey JH. New clinical test of retinal function based upon the standing potentials of the eye. Brit J Ophthal 1962, 46: 449-467.

Arden GB and Kelsey JH. Changes produced by light in the standing potential of the human eye. J Physiol 1962, 161:189-204.

Barber HO and Stockwell CW. Manual of electronystagmography. CV Mosby, St Louis, 1980.

Barlow JS and Rémond A. Eye movement artifact nulling in EEGs by multichannel on-line EOG subtraction. Electroencephalogr Clin Neurophysiol 1981, 52: 418-423.

Barry W. and Jones GM. Influence of eye lid movement upon electro-oculographic recording of vertical eye movements. Aerosp Med 1965, 36: 855-858.

Becker W and Fuchs AF. Further properties of the human saccadic system: Eye movements and correction saccades with and without visual fixation points. Vision Res 1969, 9: 1247-1258.

Becker W and Fuchs AF. Lid-eye coordination during vertical gaze changes in man and monkey. J Neurophysiol 1988, 60: 1227-1252.

Berg P. The residual after correcting event-related potentials for blink artifacts. Psychophysiol 1986, 23: 354-364.

Berg P. and Davies MB. Eyeblink-related potentials. Electroencephalogr Clin Neurophysiol 1988, 69: 1-5.

Berg P. and Scherg M. Dipole models of eye movements and blinks Electroencephalogr Clin Neurophysiol 1991a, 79: 36-44.

Berg P. and Scherg M. Dipole modelling of eye activity and its application to the removal of eye artifacts from the EEG and MEG. Clin Phys Physiol Meas 1991b, Vol. 12, Suppl. A.

Berg P, Scherg M and Braun C. Correction of EOG artifacts without distortion of spatial topography. In preparation, 1993.

Berson EL. Electrical phenomena in the retina. In: RA Moses and WM Hart (Eds), Adler's Physiology of the Eye. Clinical Application. Eighth Edition. Mosby, Toronto, 1987: 507-567.

Blinn KA. Focal and anterior temporal spikes from external rectus muscle. Electroencephalogr Clin Neurophysiol 1955, 7: 299-302.

Brazis PW, Masdeu JC and Biller J. Localization in clinical neurology. Little, Brown and Company, Boston, 1990: 209.

Brindley GS. Resting potential of the lens. Brit J Ophthal 1956, 40: 385-391.

Brittenham DM. Artifacts. In: DD Daly and TT Pedley (Eds), Current Practice of Clinical Electroencephalography. Raven Press, New York, 1990: 91-97.

Brunia CHM, Mocks J, van den Berg-Lenssen, MMC et al. Correcting ocular artifacts in the EEG: A comparison of several methods. J Psychophysiol 1989, 3: 1-50.

Caskadon MA and Rechtschaffen A. Monitoring and staging human sleep. In: HK Meir, Roth T and Dement WC (Eds), Principle and Practice of Sleep Medicine. WB Saunders Company, Philadelphia, 1989:665-683.

Coats, A.C. Electronystagmography. In: L.J. Bradford (eds.), Physiological measures of the audio-vestibular system. Academic Press, New York, 1975: 37-85.

Collewijn H, Van Der Steen J and Steinman RM. Human eye movements associated with blinks and prolonged eyelid closure. J Neurophysiol 1985, 54: 11-27.

Corby JC, Bert S and Kopell BS. Differential contributions of blinks and vertical eye movement as artifacts in EEG recording. Psychophysiol 1972, 9: 640-644.

Davson H. Physiology of the Eye. Macmillan, London, 1990: 660-661.

Doane MG. Interaction of eyelids and tears in corneal wetting and the dynamics of the normal human eyeblink. Am J ophthalmol 1980, 89: 507-516.

Donn A, Maurice DM and Mill NL. Studies on the living cornea in vitro. Arch Ophthalm 1959, 62: 741-747.

Du Bois Reymond E. Untersuchungen über tierische Elektrizität. Reimer, Berlin, 1849, 2: (1) 256.

Elbert T, Lutzenberger W, Rockstroh B and Birbaumer N. Removal of the ocular artifacts from the EEG - A biophysical approach to the EOG. Electroencephalogr Clin Neurophysiol 1985, 60: 455-463

Evinger MD, Shaw CK, Manning KA and Baker R. Blinking and associated eye movement in humans, guinea pigs and rabbits. J Neurophysiol 1984, 52: 323-38.

Fender DH. Source Localization of Brain Electrical Activity. In AS Gevins & A Rémond (Eds) Handbook of Electroencephalography and Clinical Neurophysiology. Volume 1. Methods of Analysis of Brain Electrical and Magnetic Signals. Elsevier, Amsterdam, 1987: 355-403.

Fisch BJ Spehlmann's EEG primer. Elsevier, New York, 1991.

Gasser T, Sroka L and Mocks J. The correction of EOG artifacts by frequency dependent and frequency independent methods. Psychophysiology 1986, 23: 704-712.

Geddes LA and Baker LE. Principles of applied biomedical instrumentation. Wiley, New York, 1989: 760-767.

Geddes LA. Electrodes and the measurement of bioelectric events. Wiley, New York, 1972: 102.

Gevins AS. Overview of computer analysis. In: Gevins AS and Rémond A. (Eds), Handbook of Electroencephalography and Clinical Neurophysiology. Elsevier, Amsterdam, 1987: 64-65.

Granit R. Sensory mechanisms of the retina. Oxford University Press, London, 1947.

Gratton G, Coles MGH and Donchin E. A new method for off-line removal of ocular artifact. Electroencephalogr Clin Neurophysiol 1983, 55: 468-484.

Häkkinen V, Hirvonen K, Hasan J, Kataja M, Värri A, Loula P and Eskola H. Effects of small differences in electrode positions on EOG signals. Application to vigilance studies. Electroencephalogr Clin Neurophysiol 1993, 86: 294-300.

Hector ML. EEG recording. Butterworths, London, 1976.

Hillyard SA and Galambos R. Eye movement artifact in the CNV. Electroencephalogr Clin Neurophysiol 1970, 28: 173-182.

Hughes JR and Miller JK. Eye movements on brain maps. Clin Electroencephalogr 1988, 19: 210-213.

Ifeachor EC, Jervis BW, Allen EM, Moris EL, Wright DE and Hudson NR. Investigation and comparison of some models for removing ocular artifacts from EEG signals. Med Biol Eng Comput 1988, 26: 584-590; 591-598.

Jacobson E. Electrical measurements of neuromuscular states during mental activities. Am J Psychol 1930, 95: 694-702.

Jervis BW, Nichols MJ, Allen EM, Hudson NR and Johnson TE. The assessment of two methods for removing eye movement artifact from the EEG. Electroncephalogr Clin Neurophysiol 1985, 61: 444-452.

Jervis BW, Ifeachor EC and Allen EM. The removal of ocular artifacts from the electroencephalogram: a review. Med Biol Eng Comput 1988, 26: 2-12.

John ER, Harmony T and Valdes-Sosa P. The uses of statistics in electrophysiology. In: Gevins AS and Rémond A. (Eds), Handbook of Electroencephalography and Clinical Neurophysiology. Elsevier, Amsterdam, 1987: 527-529.

Kiloh LG, McComas AJ, Osselton JW and Upton ARM. Clinical electroencephalography. Butterworths, London, 1981.

Krogh E. Normal values in clinical electrooculography. I. Materials, method, methodological investigations and distribution of the potential and time parameters. Acta Opthal 1975, 53: 563-575.

Krogh E. Normal values in clinical electrooculography. II. Analysis of potential and time parameters and their relation to other variables. Acta Opthal 1976, 54: 389-400.

Kurtzberg D and Vaughan HG. Topographic analysis of human cortical potentials preceding self-initiated and visually triggered saccades. Brain Res 1982, 243: 1-9

Lasansky A and de Fisch FW. Potential, current and ionic fluxes across the isolated retinal pigment epithelium and choroid. J Gen Physiol 1966, 49: 913-24.

Lee S. and Buchsbaum MS. Topographic mapping of EOG artifacts. Clin Electroencephalogr 1987, 18: 61-67.

Marg E. Development of electro-oculography. Arch Ophthalmol 1951, 45: 169-185.

Marton M, Szirtes J, Donauer N and Breuer P. Saccade-related brain potentials in semantic categorization tasks. Biol Psych 1985, 20: 163-184.

Matsuo F, Peters, JF and Reilly EL. Electrical phenomena associated with movements of the eyelid. Electroncephalogr Clin Neurophysiol 1975, 38: 507-511.

McCallum WC and Walter WG. The effects of attention and distraction on the contigent negative variation in normal and neurotic subjects. Electroencephalogr Clin Neurophysiol 1968, 25: 319-329.

McCloskey DI. Corollary discharges: motor commands and perception. VB Brooks (Ed), Handbook of Physiology. Section 1: The Nervous System. Volume II. Motor Control, Part 2. Maryland, Bethesda, American Physiology Society, 1981, 1415-1447.

Meyers IL. Electronystagmography. A graphic study of the action currents in nystagmus. Arch Neurol and Psychiat 1929, 21: 901-918.

Miyauchi S, Takino R, Fukuda H and Torii S. Electrophysiological evidence for dreaming: human cerebral potentials associated with rapid eye movements during REM sleep. Electroencephalogr Clin Neurophysiol 1987, 66: 383-390.

Möcks J and Verlenger R. Multivariate methods in biosignal analysis: application of principal component analysis to event-related potentials. In Weitkunat R (Ed)

Digital Biosignal Processing. Techniques in the Behavioral and Neural Sciences. Vol 5. Amsterdam, Elsevier, 1991: 399-458.

Moses RA. Adler's Physiology of the eyes. Clinical application. CV Mosby, St Louis, 1970.

Mowrer OH, Ruch TC and Miller NE.. The corneo-retinal potential difference as the basis of the galvanometric method of recording eye movements. Am J Physiol 1936; 114:423-428.

Müller-Limmroth H and Lemaître M. Über das Bestandpotential des Auges und seine Beziehungen zum Elektroretinogramm. Z Biol 1953, 105:348-362.

Näätänen R and Picton TW. The N1 wave of the human electric and magnetic response to sound: a review and analysis of the component structure. Psychophysiol 1987, 24: 375-425.

Nunez PL and Katznelson RD. Electric fields of the brain: the neurophysics of EEG. Oxford, New York, 1981.

Pasik P, Pasik T and Bender MB. Recovery of the electro-oculogram after total ablation of the retina in monkeys. Electroencephalogr Clin Neurophysiol 1965, 19: 291-297.

Picton TW and Hillyard SA. Cephalic skin potentials in electroencephalography. Electroencephalogr Clin Neurophysiol 1972, 33: 419-424.

Picton TW. The recording and measurement of evoked potentials. In: AM Halliday, SR Butler and R Paul (Eds), Textbook of clinical neurophysiology. Wiley, Chichester, 1987.

Picton TW. Auditory Evoked Potentials. In: DD Dale and TA Pedley (Eds), Current Practice of Clinical Electroencephalography. Raven Press, New York, NY, 1990:625-678.

Rechtschaffen A and Kales A (eds), A Manual of Standardized Terminology: Techniques and Scoring System for Sleep Stages of Human Subjects. UCLA Brain Information Service/Brain Research Institute, Los Angeles, 1968.

Scherg M and von Cramon D. Two bilateral sources of the late AEP as identified by a spatio-temporal dipole model. Electroencephalogr Clin Neurophysiol 1985, 62: 344-360.

Scherg M and von Cramon D. Evoked dipole source potentials of the human auditory cortex. Electroencephalogr Clin Neurophysiol 1986, 65: 344-360.

Scherg M. Fundamentals of dipole source analysis. In: M Hoke, F Grandori and GL Romani (eds) Advances in Audiology, Vol 6. Auditory Evoked Magnetic Fields and Potentials. Basel, Karger, 1990: 40-69

Scherg M and Picton TW. Separation and identification of event-related potential components by brain electric source analysis. In: CHM Brunia, G Mulder and MN Verbaten (eds) Event-related Potentials of the Brain. Electroencephalogr Clin Neurophysiol, Suppl. 42, Elsevier, Amsterdam, 1991: 24-37.

Scherg M. Functional imaging and localization of electromagnetic brain activity. Brain Topography, in press

Semlitsch HV, Anderer P, Schuster P and Presslich O. A solution for reliable and valid reduction of ocular artifacts, applied to the P300 ERP. Psychophysiol 1986, 23: 965-703.

Spelhlmann R. EEG primer. Elsevier Biomedical Press, Amsterdam, 1981: 105-109.

Steinberg RH, Linsenmeier RA and Griff ER. Three light-evoked responses of the retinal pigment epithelium. Vision Res 1983, 23: 1315-1323.

Stephenson SA and Gibbs FA. A balanced noncephalic reference electrode. Electroencephalogr Clin Neurophysiol 1951, 3: 237-240.

Stern JA, Walrath LC and Goldstein R. The endogenous eyeblink. Psychophysiol 1984, 21: 22-33.

Tabachnick BG and Fidell LS. Using Multivariate Statistics. Harper Collins Publishers, Northridge, 1989: 597-600.

Verleger R. The instruction to refrain from blinking affects auditory P3 and N1 amplitudes. Electroencephalogr Clin Neurophysiol 1991, 78: 240-251.

Whitton JL, Lue F and Moldofsky H. A spectral method for removing eye movement artifacts from the EEG. Electroencephalogr Clin Neurophysiol 1978, 44: 735-741.

Wilkins RH and Brody IA. Bell's palsy and Bell's phenomenon. Arch Neurol 1969, 21: 661-662.

Wood CC. Application of dipole localization methods to source identification of human evoked potentials. Ann NY Acad Sci 1982, 388: 139-155.

Yagi A. Visual signal detection and lambda responses. Electroencephalogr Clin Neurophysiol 1981, 52: 604-610.

Zao ZZ, Gelbin J and Rémond A. Le champ électrique de l'oiel. Sem Hôp Paris 1952, 36: 1506-1513.

STATISTICAL COMPARISONS

SUMMARY TABLES

Age in males and females

Two-group t-test

measurement	t	df
age	0.46	10

Head measurements in males and females

Two-group t-test

measurement	t	df
inion-nasion	2.05	10
inter-preauricular	2.05	10
circumference	2.17	10

Blink parameters correlated with head measurements

Pearson product-moment correlation coefficients.

	head measurement →	inion-nasion	inter-auricular	circumference
measurement	blink	r	r	r
amplitude	natural	-0.237	-0.178	-0.237
	voluntary	-0.048	0.029	-0.155
total duration	natural	0.38	0.475	0.263
	voluntary	-0.16	-0.121	-0.210
half-amplitude duration	natural	0.127	0.222	0.061
	voluntary	-0.238	-0.160	-0.214

Blink onset-to-peak and peak-to-end durations

Paired t-test

measurement	blink	t	df
onset to peak versus peak to end	natural	-3.72	11
	voluntary	-8.53	11

Blink parameters in natural blinks and voluntary blinks

Paired t-test

measurement		t	df
duration	total	0.87	11
	onset to peak	0.58	11
	peak to end	0.45	11
	half amplitude	-2.29*	11
amplitude	peak	-2.41*	11

* $p \leq 0.01$

Bonferroni adjusted t= 0.01 for alpha = 0.01

Blink parameters in males and females

Two-group t-test

measurements		blink	t	df
duration	total	natural	-1.17	10
		voluntary	-0.68	10
	onset to peak	natural	-1.96	10
		voluntary	-0.68	10
	peak to end	natural	-0.25	10
		voluntary	-0.43	10
	half-amplitude	natural	-1.74	10
		voluntary	-0.80	10
amplitude	peak	natural	0.42	10
		voluntary	1.32	10

Rate of change of potentials at the onset and offset of natural and voluntary blinks

Two-way analysis of variance: blink (natural and voluntary) by segment (Onset: 100ms preceding blink peak; offset: 100 ms following peak)

source of variance	SS	df	MS	F
Blink	6.187500	1	6.187500	3.75
error	16.514999	10	1.651500	
Segment	20.865681	1	20.865681	135.77*
error	1.536818	10	0.153682	
BS	1.565683	1	1.565682	23.84*
error	0.656818	10	0.065682	

Simple main effects for the blink by segment interaction: blink at segment

source of variance	SS	df	MS	F
blink at onset	6.989092	1	6.989092	6.80*
error	10.270909	10	1.027091	
blink at offset	0.764091	1	0.764091	1.11
error	6.900908	10	0.690091	

* $p < 0.05$

Rate of change of potentials at the onset of natural blinks, voluntary blinks and up saccades

One-way analysis of variance: artifact (natural blink, voluntary blink and up saccade)

source of variance	SS	df	MS	F
artifact	47.9465	1	47.9465	4.50
error	117.0911	11	10.6446	

Vertical propagation factors of natural and voluntary blinks

Three-way analysis of variance: condition (natural and voluntary blinks) by position (pre-frontal, anterio-temporal, frontal, mid-temporal, central, posterio-temporal, parietal and occipital) by side (right and left)

source of variance	SS	df	MS	F
Condition	0.000092	1	0.000037	0.03
error	0.038269	11	0.003479	
Position	7.91439	8	0.989299	305.89*1
error	0.284607	88	0.003234	
Side	0.004288	1	0.004288	4.1
error	0.0115	11	0.001045	
CP	0.00099	8	0.000124	0.66
error	0.016477	88	0.000197	
CS	0.00045	1	0.00045	1.83
error	0.002712	11	0.000247	
PS	0.015795	8	0.001974	3.74*2
error	0.046418	88	0.000527	
CPS	0.001018	8	0.000127	1.35
error	0.008312	33	0.000094	

Simple main effects for the position by side interaction: side at positions

source of variance	SS	df	MS	F
side at frontopolar	0.018408	1	0.018408	5.14 *
error	0.039363	11	0.003578	
side at anterio-temporal	0.00052	1	0.00052	0.65
error	0.008751	11	0.000796	
side at frontal	0.001008	1	0.001008	2.57
error	0.004314	11	0.000392	
side at earlobe	0.000044	1	0.000044	1.31
error	0.000369	11	0.000034	
side at mid-temporal	0.000015	1	0.000015	0.31
error	0.000534	11	0.000049	
side at central	0.000004	1	0.000004	0.06
error	0.000769	11	0.00007	
side at posterio-temporal	0.000052	1	0.000052	1.84
error	0.000311	11	0.000028	
side at parietal	0.000024	1	0.000024	0.36
error	0.000727	11	0.000066	
side at occipital	0.000007	1	0.000007	0.03
error	0.002782	11	0.000253	

* $p < 0.05$

*1 Geisser-Greenhouse adjusted df = 2.08, $p < 0.05$

*2 Geisser-Greenhouse adjusted df = 1.61, $p < 0.05$

Saccade amplitudes correlated with head measurements

Pearson product-moment correlation coefficients. Measurements performed at the EOG channels.

head measurement →	inion-nasion	inter-auricular	circumference
20 degrees saccade	r	r	r
vertical	0.1	0.069	-0.229
horizontal	-0.398	-0.492	

Saccade amplitudes in males and females.

Two-group t-test. Measurements performed at the EOG channels.

20 degree saccades	t	df
vertical	0.43	10
horizontal	-1.34	10

Amplitudes of up, down, left and right 20 degree saccades.

Two-way analysis of variance: orientation (vertical and horizontal) by direction (up or right and down or left). Vertical saccades were measured at the vertical EOG and horizontal saccades at the horizontal EOG channel.

Source of Variance	SS	df	MS	F
Orientation	102028.5	1	102028.5	9.67 *
error	116091.7	11	10553.79	
Direction	346.6875	1	346.6875	0.3
error	12573.56	11	1143.051	
OD	238.5208	1	238.5208	0.43
error	6136.729	11	557.8845	

* $p < 0.05$.

Durations of up, down, right and left 20 degrees saccades.

Two-way analysis of variance: orientation (vertical and horizontal) by direction (up or right and down or left). Vertical saccades were measured at the vertical EOG and horizontal saccades at the horizontal EOG channel.

Source of Variance	SS	df	MS	F
Orientation	720.4861	1	720.4861	0.7
error	11233.33	11	1021.212	
Direction	464.5778	1	464.5778	0.4
error	13614.56	11	1237.636	
DA	294.5673	1	294.5673	0.3
error	9367.683	11	851.6075	

Vertical propagation factors of 20 and 10 degree saccades

Three-way analysis of variance: condition (20 and 10 degrees saccades) by position ((pre-frontal, anterio-temporal, frontal, mid-temporal, central, posterio-temporal, parietal and occipital) by side (right and left).

source of variance	SS	df	MS	F
Condition	0.000612	1	0.000612	0.04
error	0.174433	11	0.015858	
Position	6.704848	8	0.838106	179.55 *1
error	0.41076	88	0.004668	
Side	0.004082	1	0.004082	2.56
error	0.017572	11	0.001597	
CP	0.050887	8	0.006361	5.09 *2
error	0.109889	88	0.001249	
CS	0.000721	1	0.000721	1.27
error	0.00624	11	0.000567	
PS	0.018803	8	0.00235	3.29
error	0.062788	88	0.000714	
CPS	0.001649	8	0.000206	0.58
error	0.031463	88	0.000358	

Simple main effects for the condition by position interaction: conditions at positions.

Source of Variance	SS	df	MS	F
condition at frontopolar	0.027028	1	0.27028	4.16
error	0.071484	11	0.006499	
condition at anterio-temporal	0.01197	1	0.011977	4.18
error	0.031478	11	0.002862	
condition at frontal	0.001045	1	0.001045	0.54
error	0.021206	11	0.001928	
condition at earlobe	0.000252	1	0.000252	1.16
error	0.002397	11	0.000279	
condition at mid-temporal	0.000137	1	0.000137	0.08
error	0.018491	11	0.001681	
condition at central	0.001863	1	0.001863	1.08
error	0.018992	11	0.001727	
condition at posterio-temporal	0.000736	1	0.000736	0.25
error	0.032473	11	0.002952	
condition at parietal	0.001888	1	0.001888	0.4
error	0.052542	11	0.004777	
condition at occipital	0.00658	1	0.00658	2.05
error	0.035261	11	0.035261	

Vertical propagation factors of up and down saccades

Three-way analysis of variance: condition (up and down 20 degree saccades) by position (pre-frontal, anterio-temporal, frontal, mid-temporal, central, posterio-temporal, parietal and occipital) by side (right and left)

Source of Variance	SS	df	MS	F
Condition	0.006015	1	0.006015	0.72
error	0.091955	11	0.00836	
Position	6.002313	8	0.750289	147.04 *
error	0.449023	88	0.005103	
Side	0.001193	1	0.001193	0.8
error	0.016506	11	0.001501	
CP	0.014896	8	0.001862	0.68
error	0.239834	88	0.002725	
CS	0.002465	1	0.002465	2.42
error	0.011209	11	0.001019	
PS	0.015218	8	0.001902	2.23
error	0.075204	88	0.000855	
CPS	0.001639	8	0.000205	0.51
error	0.035016	88	0.000398	

* Geisser-Greenhouse: adjusted df = 2.86; $p < 0.05$

Vertical propagation factors of saccades and blinks

Two-way analysis of variance: condition (overall 20/10 degree saccades and overall natural/voluntary blinks) by position (Fp1/2, F7/8, F3/4, FZ, A1/2, T3/4, C3/4, CZ, T5/6, P3/4, PZ, 01/2)

Source of Variance	SS	df	MS	F
Condition	0.004583	1	0.004583	7.02 *
error	0.77728	11	0.0006527	
Position	3.963859	12	0.330322	233.36 *1
error	0.186845	132	0.001415	
CP	0.015379	12	0.0011282	5.63 *2
error	0.030026	132	0.0002275	

Simple main effects for the condition by position interaction: conditions at positions.

source of variance	SS	df	MS	F
Condition at Fp1-2	0.003781	1	0.003781	4.2
error	0.009896	11	0.0009	
Condition at F7-8	0.001183	1	0.001183	4.02
error	0.003235	11	0.000294	
Condition at F3-4	0.000138	1	0.000138	0.54
error	0.027931	11	0.000254	
Condition at FZ	0.00036	1	0.00036	2.01
error	0.001973	11	0.000179	
Condition at A1-2	0.000002	1	0.000002	0.04
error	0.000735	11	0.000067	
Condition at T3-4	0.000045	1	0.000045	0.3
error	0.001649	11	0.00015	
Condition at C3-4	0.001376	1	0.001376	8.06 *
error	0.001879	11	0.000171	
Condition at CZ	0.002176	1	0.002176	11.53 *
error	0.002075	11	0.000189	
Condition at T5-6	0.001121	1	0.001121	5.78 *
error	0.002132	11	0.000194	
Condition at P3-4	0.001913	1	0.001913	8.17 *
error	0.002575	11	0.000234	
Condition at PZ	0.005475	1	0.005475	11.67 *
error	0.005160	11	0.005161	
Condition at O1-2	0.001094	1	0.001094	7 *
error	0.001718	11	0.000156	
Condition at OZ	0.001298	1	0.001298	10.3 *
error	0.001386	11	0.000126	

* $p < 0.05$.

*1 Geisser-Greenhouse: adjusted df = 2.39; $p < 0.05$

*2 Geisser-Greenhouse: adjusted df = 1.64; $p < 0.05$

Horizontal propagation factors of 20 and 10 degree saccades

Three-way analysis of variance: Condition (20 and 10 degree saccades) by position (pre-frontal, anterio-temporal, frontal, mid-temporal, central, posterio-temporal, parietal and occipital) by side (right and left). Propagation factors are expressed in absolute values.

Source of Variance	SS	df	MS	F
Condition	0.002966	1	0.002966	1.58
error	0.020612	11	0.001874	
Position	1.301293	8	0.162662	89.64 *1
error	0.159679	88	0.001815	
Side	0.006502	1	0.006502	0.59
error	0.121887	11	0.011081	
CP	0.007509	8	0.000939	0 81
error	0.102035	88	0.001159	
CS	0.025331	1	0.025331	5.26 *
error	0.052957	11	0.004814	
PS	0.007645	8	0.000956	0.72
error	0.116127	88	0.00132	
CPS	0.034725	8	0.004341	7.18 *2
error	0.053201	88	0.000605	

Simple main effects for the condition by position by side interaction: side by position at condition

Source of Variance	SS	df	MS	F
20° Saccades	0.016257	8	0.002032	1.82
error	0.098302	88	0.001117	
10° Saccades	0.026113	8	0.003264	4.04 *3
error	0.071025	88	0.000807	

Simple main effects for the condition by position by side interaction: condition by position at side

Source of Variance	SS	df	MS	F
Right	0.029717	8	0.003715	4.29 *4
error	0.076125	88	0.000865	
Left	0.012516	8	0.001565	1.74
error	0.079111	88	0.000899	

Simple-simple main effects for the condition by position at right side interaction

Source of Variance	SS	df	MS	F
Frontopolar	0.014652	1	0.04652	4.13
error	0.039046	11	0.00355	
Anterio-Temporal	0.0149	1	0.0149	7.37 *
error	0.022227	11	0.002021	
Frontal	0.009923	1	0.009923	7.96 *
error	0.013718	11	0.001247	
Earlobe	0.001107	1	0.001107	2
error	0.00608	11	0.000553	
Mid-Temporal	0.005953	1	0.005953	5.34 *
error	0.012258	11	0.001114	
Central	0.004161	1	0.004161	3.28
error	0.013935	11	0.001267	
Posterio-Temporal	0.001473	1	0.001473	4.19
error	0.003865	11	0.000351	
Parietal	0.000092	1	0.000092	0.19
error	0.005282	11	0.00048	
Occipital	0.000273	1	0.000273	0.57
error	0.005308	11	0.000483	

Simple-simple main effects for the side by position at 10 degree saccades interaction

Source of Variance	SS	df	MS	F
Frontopolar	0.00152	1	0.00152	0.72
error	0.023283	11	0.002117	
Anterio-Temporal	0.02754	1	0.02754	15.41 *
error	0.019665	11	0.001788	
Frontal	0.013776	1	0.13776	6.3 *
error	0.006042	11	0.000549	
Earlobe	0.001883	1	0.001803	1.57
error	0.012634	11	0.001149	
Mid-Temporal	0.006767	1	0.006767	4.11
error	0.018095	11	0.001645	
Central	0.00329	1	0.00329	2.51
error	0.014441	11	0.001313	
Posterio-Temporal	0.000008	1	0.00008	0.01
error	0.008691	11	0.00079	
Parietal	0.000067	1	0.000067	0.09
error	0.008348	11	0.000759	
Occipital	0.000092	1	0.000092	0.22
error	0.004669	11	0.000425	

* $p < 0.05$

*1 Geisser-Greenhouse: adjusted df = 2.32; $p < 0.05$

*2 Geisser-Greenhouse: adjusted df = 2.71; $p = 0.05$

*3 Geisser-Greenhouse: adjusted df = 2.25; $p < 0.05$.

*4 Geisser-Greenhouse: adjusted df = 1.88; $p < 0.05$.

Horizontal propagation factors of right and left saccades

Three-way analysis of variance: condition (right and left 20 degree saccades) by position (pre-frontal, anterio-temporal, frontal, mid-temporal, central, posterio-temporal, parietal and occipital) by side (right and left)

Source of Variance	SS	df	MS	F
Condition	0.012256	1	0.012256	13.73 *
error	0.009817	11	0.000892	
Position	1.384509	8	0.173064	94.54 *1
error	0.161084	88	0.001831	
Side	0.010199	1	0.010199	0.77
error	0.14553	11	0.01323	
CP	0.011059	8	0.001382	3.65 *2
error	0.033342	88	0.000379	
CS	0.001716	1	0.001716	0.46
error	0.041115	11	0.003738	
PS	0.004527	8	0.000566	0.32
error	0.15531	88	0.001765	
CPS	0.017486	8	0.002186	3.4 *3
error				

Simple main effects for the condition by position by side interaction: side by position at condition

Source of Variance	SS	df	MS	F
right saccades	0.007651	8	0.000956	0.67
error	0.126115	88	0.001433	
left Saccades	0.014362	8	0.001795	1.84
error	0.085789	88	0.000975	

Simple main effects for the condition by position by side interaction: condition by position at side

Source of Variance	SS	df	MS	F
Right	0.017655	8	0.002207	4.85 *4
error		88		
Left	0.01089	8	0.001361	2.4
error	0.049915	88	0.000567	

Simple-simple main effects for the condition by position at right side interaction

Source of Variance	SS	df	MS	F
Frontopolar	0.002817	1	0.002817	2.32
error	0.013370	11	0.001215	
Anterio-Temporal	0.018928	1	0.018928	12.24 *
error	0.017012	11	0.001547	
Frontal	0.003626	1	0.003626	4.06
error	0.00982	11	0.000893	
Earlobe	0.00021	1	0.00021	0.32
error	0.007331	11	0.000667	
Mid-Temporal	0.001504	1	0.001504	2.25
error	0.007357	11	0.000669	
Central	0.001584	1	0.001584	4.72
error	0.003694	11	0.000336	
Posterio-Temporal	0.000376	1	0.000376	1.31
error	0.003155	11	0.000287	
Parietal	0.000108	1	0.000108	0.65
error	0.001837	11	0.000167	
Occipital	0.000074	1	0.000074	0.25
error	0.003272	11	0.000297	

* $p < 0.05$
*1 Geisser-Greenhouse: adjusted df = 2.64;$p < 0.05$.
*2 Geisser-Greenhouse: adjusted df = 3.16;$p < 0.05$
*3 Geisser-Greenhouse: adjusted df = 2.67;$p < 0.05$
*4 Geisser-Greenhouse: adjusted df = 3.99; $p < 0.05$.

Blinks and saccades propagation factors correlated with head measurements

Pearson product-moment correlation coefficients.

head measurement →		inion-nasion	inter-auricular	circumference
artifact	**location**	**r**	**r**	**r**
natural blinks	FZ	0.09	0.1	-0.02
	CZ	0.3	0.31	0.44
vertical saccades	FZ	-0.1	-0.23	-0.18
	CZ	-0.2	-0.22	-0.18
horizontal saccades	F7/8	-0.51	-0.55	-0.54
	T3/4	0.09	-0.6 *	-0.51

* $p < 0.05$

Horizontal propagation factors of horizontal saccades, smooth pursuit and reading

Two-way analysis of variance: condition (horizontal saccades, smooth pursuit eye movements and eye movement during reading) by position (F7, F8, T3, T4, T5, T6, O1 and O2)

Source of Variance	SS	df	MS	F
Condition	0.011921	2	0.00596	4.24
error	0.011236	14	0.001404	
Position	1.672216	7	0.238888	91.94 *
error	0.072749	28	0.002598	
CP	0.009163	14	0.000654	1.11
error	0.033078	56	0.000591	

* Geisser-Greenhouse adjusted df = 1.15; $p < 0.05$

Amplitudes of the "test" waveforms corrected with the studied correction methods

Two-way analysis of variance: method (regression-1, regression-2, dipole, PCA-1 and PCA-2) by position (FZ, T3, CZ, T4, and PZ). Amplitudes are the root-mean-square of the corrected waveforms

Source of Variance	SS	df	MS	F
method	197.463984	4	49.365996	7.88 *
error	150.301444	24	6.226256	
position	78.692472	4	19.673118	1.68
error	280.72318	24	11.696799	
MP	26.883571	16	1.680223	0.97
error	165.870898	96	1.727882	

Tukey HSD post-hoc comparisons for the significant main effect for method

Method	mean	PCA-3	dipole	regression-2	regression-1
PCA-1	5.6688	0.0174	0.4298	1.8213	2.6366 *
PCA-3	5.6862	—	0.4224	1.8039	2.6192 *
dipole	6.0986		—	1.3915	2.2068 *
regression-2	7.4901			—	0.8152
regression-1	8.3054				—

* $p < 0.05$